

Investigation of the Scarcity of Intervention Programs for Late Adolescents Dealing with Parental Incarceration

Darynne Madison (Madi) Dela Gente¹

¹USC Keck School of Medicine Department of Population and Public Health Sciences

Abstract:

The United States has the world's highest incarceration rate, with a significant portion of these individuals having adolescent children [1]. Adolescents dealing with parental incarceration are more likely to experience financial instability, engage in risky behaviors such as substance abuse, sexual activity, crime, and delinquency, and are also at higher risk of dropping out of school [2]. Associated health outcomes include depression, PTSD, anxiety, interpersonal, and behavioral issues [3]. Although there are several intervention programs available to limit these consequences, they primarily target early and middle stages of adolescence (ages 10-17) and ultimately lack attention towards the later stages of adolescence (ages 18-21) [4]. A web search examination using major search engines, examined both the quantity and quality of intervention programs within the United States. The analyses revealed a dire need for support for late adolescents, in contrast to an abundance of resources for early and middle adolescents. Intervention program trends were then utilized to generate a hypothetical intervention program model that takes into account developmental differences between early, middle, and late adolescents.

Introduction:

Incarceration is a highly consequential issue within the United States, having economic, social, and ethical repercussions on staff, inmates, and in particular, their family members. Within the United States, approximately 1.9 million people are incarcerated [5]. It is estimated that 2.7 million adolescents have experienced having

at least one parent incarcerated [6]. Due to the understudied, overlooked, and heavily stigmatized nature of the issue of parental incarceration, this subset population of adolescents are often coined "hidden victims". Existing research has determined that parental incarceration has a myriad of consequences for adolescents. Within the health sector, adolescents are more likely to struggle with mental health (i.e. depression, PTSD, anxiety, increased stress levels) and possess interpersonal issues (i.e. anti-social tendencies) [3]. From an academic standpoint, this population has a higher risk of dropping out, having a learning disability, a decreased rate of cognitive skills, and a lower likelihood of attaining higher education [2]. Risks for these adolescents also include intergenerational incarceration through engagement in criminal activity, substance abuse, heightened sexual behavior, and increased rates of delinquency [2]. It is because of these consequences, that the Center for Disease Control and Prevention has declared parental incarceration an "Adverse Childhood Experience (ACE)", which is defined as a traumatic childhood event that negatively influences an adolescent's health and wellbeing. Surmounting consequences have prompted organizations across the nation to establish intervention programs to mitigate the effects of these negative outcomes. This study investigates implemented intervention programs and its offered services, as well as overall availability for the three developmental stages of adolescence, which is defined as early (ages 10-14), middle (ages 15-17), and late (ages 18-21) [4].

Materials and Methods:

A. Quantitative & Qualitative Evaluation of Currently Implemented Intervention Programs

Search parameters regarding the age range of the three stages of adolescents, were input into major search engines to observe the quantity of search results relative to each phrase. Accessibility was then determined by recording the sum of available intervention programs within each of the 50 states, regardless of an adolescent age range constraint. Data from the Annie E. Casey Foundation was utilized to provide a statewide demographic gauge of how many adolescents are dealing with parental incarceration. The foundation obtained data via KIDS COUNT Data Centers, 50 state-level organizations that specifically collect data regarding the wellbeing of families and adolescents. Intervention programs were quantified by state availability by inputting the key words “Parental incarceration programs [state name]”. Nationwide databases, such as The National Resource Center on Children and Families of the Incarcerated, were also consulted to cultivate the most comprehensive quantification. The search was then narrowed to the targeting of adolescent group age ranges (10-17 and 18-21), where both the quantity, quality, and age-specific services were studied. Quality of intervention programs was first determined by analyzing the type of services offered (i.e. activities for youth, economic and health related resources, discussion spaces, mentors etc.), accessibility (in-person vs virtual, free programs), and specificity (programs specifically for youth with a parent in prison). Programs were then classified as early, middle, or late adolescent specific based on age restriction or the age appropriateness of the services. For the late adolescent group, both local and collegiate programs—those that are offered through a college/university for undergraduates undergoing parental incarceration explicitly—were examined. Inclusion criteria is as follows: intervention

programs with initiatives or projects through non-profit, governmental, or religious organizations that work towards improving the wellbeing of adolescents who have at least one parent incarcerated. Both virtual and in-person programs were included. Initiatives that provided education programs and re-entry assistance programs for incarcerated parents, despite having some direct benefits for their children, were excluded. Programs that dealt with general sectors of adolescents in difficult circumstances and did not explicitly state that they would specifically be serving adolescents with a parent incarcerated, were also excluded. All programs analyzed were found to be free for the youth. An incognito browser on a standard laptop was used to avert results that may have appeared due to the laptop’s personal search algorithm.

B. Modeling Effective Intervention Programs

Further analysis of the resources and impacts of currently implemented intervention programs revealed trends amongst offered services and their influences on its efficacy. Overlaps in offered services across all intervention programs targeting early and middle adolescents reveal the most valuable approaches in combating the consequences of parental incarceration. From these overlaps, a general model for a parental incarceration program for early and middle adolescents was developed. Taking into account the successes of early and middle adolescent intervention programs, in addition to the distinct obstacles and developmental differences of late adolescents, a hypothetical model for a late adolescent intervention program was developed.

Results:

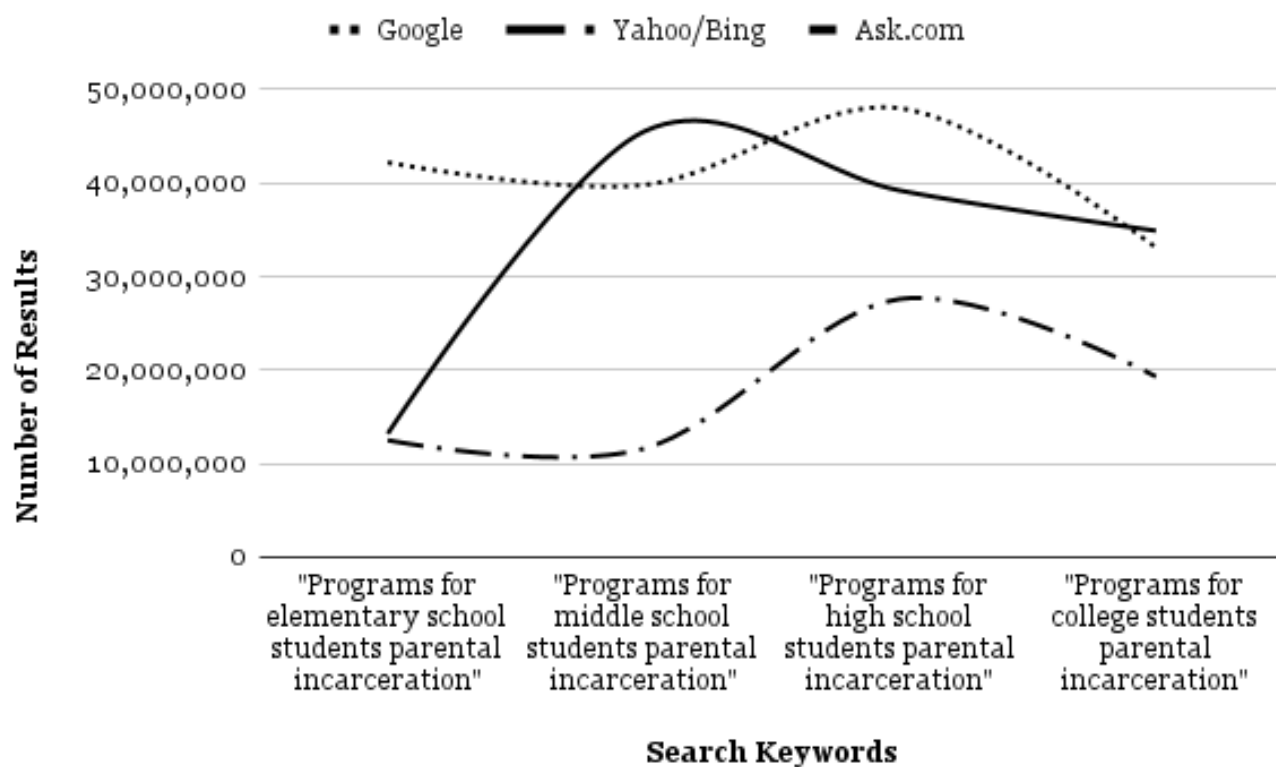


Figure 1. Number of search hits relative to search phrases specific to the three stages of adolescence.

Figure 1 exhibits a consistent downward trajectory across all major search engines when search inputs utilized keywords that indicated later stages of adolescence, such as “college students”. Analogous phrases that correlated to school groupings (i.e. “ages 5-10” for elementary school, “11-13” for middle school, etc.), though not shown on the graph, were also employed and yielded the same results. Google, Yahoo, and Bing experienced a peak with “high school” search parameters, with 40,000,000 and 20,000,000 search results respectively, while Ask.com exhibited a peak at “middle school” search parameters, with 47,000,000 search results. Quantitative differences between peak search results and search results for late adolescents were determined by taking the average number of results for peak and late adolescents (35,000,000; 34,000,000; 19,000,000) and then subtracted. Peak searches yielded 6,000,000 more results than search results for late adolescents, across all search engines.

Of the 50 states, Massachusetts, Delaware, and West Virginia offered no programs aimed at adolescents with an incarcerated parent. 60% of states offered five or more statewide programs. Florida, California, Illinois, Texas, Pennsylvania, Oregon, and Arizona, respectively, offered the greatest number of programs. Table 1 indicates a distinct relation between having a higher number of reported adolescents with a parent incarcerated resulting in a greater number of programs offered. The nationwide average of offered programs was six. This particular set of data was not exclusive to the stage of adolescence it targeted. Any and all programs, whether they were aimed for early, middle, or late adolescents, were taken into account in order to gauge accessibility.

Of the results from **Table 1**, only five states offered local/collegiate programs explicitly for late adolescent groups. On both a national and state level, the most common form of support was college scholarship funds, as shown by **Table 2**.

	Number of available parental incarceration intervention programs by state	Number of adolescents who have a parent incarcerated (2020-2021)^a
West		
Alaska	8	14,699
Arizona	11	129,998
California	12	379,495
Colorado	3	84,584
Hawaii	6	9,369
Idaho	3	33,684
Montana	5	25,058
Nevada	6	50,800
New Mexico	3	46,466
Oregon	11	44,055
Utah	7	35,965
Washington	4	84,949
Wyoming	2	14,357
Midwest		
Illinois	12	139,719
Indiana	10	152,039
Iowa	7	50,677
Kansas	6	51,318
Michigan	6	154,736
Minnesota	4	36,915
Missouri	8	134,927
Nebraska	2	25,791
North Dakota	1	12,517
Ohio	7	220,105
South Dakota	2	17,268
Wisconsin	5	100,593
Northeast		
Connecticut	3	35,549
Maine	2	14,582
Massachusetts	0	34,962
New Hampshire	5	14,893
New Jersey	1	51,442
New York	8	111,635
Pennsylvania	11	150,328
Rhode Island	4	6,988
Vermont	5	6,418
South		
Alabama	4	91,333
Arkansas	7	72,655
Delaware	0	14,099
the District of Columbia	3	4,145
Florida	15	266,711
Georgia	10	185,564
Kentucky	5	119,618
Louisiana	4	85,902
Maryland	6	67,628
Mississippi	6	56,287
North Carolina	8	146,226
Oklahoma	5	88,931
South Carolina	4	99,074
Tennessee	8	162,351
Texas	12	386,603
Virginia	7	104,760
West Virginia	0	35,207

^aData taken from the Annie E. Casey Foundation's "KIDS COUNT" Data Center

Table 1. Statewide accessibility to parental incarceration intervention programs by regions in the United States.

	Service	State/Collegiate Affiliation
Give Something Back	Financial aid assistance Mentoring Career Coaching	Nationwide
ScholarCHIPS	\$2,500 scholarship + \$250 book award Support network and mentoring	Nationwide
Hallam Law Group Scholarship	\$1,000 scholarship	Nationwide
Venus Morris Griffin Scholarship Fund	\$10,000 scholarship	Nationwide
The Children of Inmates Scholarship Fund	\$250 scholarship	Nationwide
Pitzer Family Education Foundation	Undisclosed amount	Nationwide
Ava's Grace Scholarship Foundation	\$5,000 scholarship	Missouri
Willie the Plumber Scholarship Fund	\$750 scholarship	Utah
Connecticut Children with Incarcerated Parents	Undisclosed amount	University of Connecticut
CIP Initiative	\$1500 scholarship	Central Connecticut State University
Supporting Children of Incarcerated Parents	Support group	University of Mississippi
Youth Empowerment Program	Support group	Rowan University (NJ)

Table 2. Nationwide services available to late adolescents.

There is only one reported mentoring program and two reported collegiate support groups. Average age restriction range for intervention programs was calculated by recording the age restrictions across all interventions and taking the average of the youngest and oldest age, which resulted in ages 5-17 (**Table 1**). Prisons may operate independent programs that increase engagement between inmates and their children. These are often unpublished programs due to privacy reasons, meaning

that they were not taken into account during the quantification portion of the study. The numbers presented in **Table 1** are a general approximation.

Evidence based outcomes were used to determine the success of the intervention programs amongst early and middle adolescents. Commonalities between services offered by the majority of established programs were derived and applied to cultivate a general model for a successful intervention.

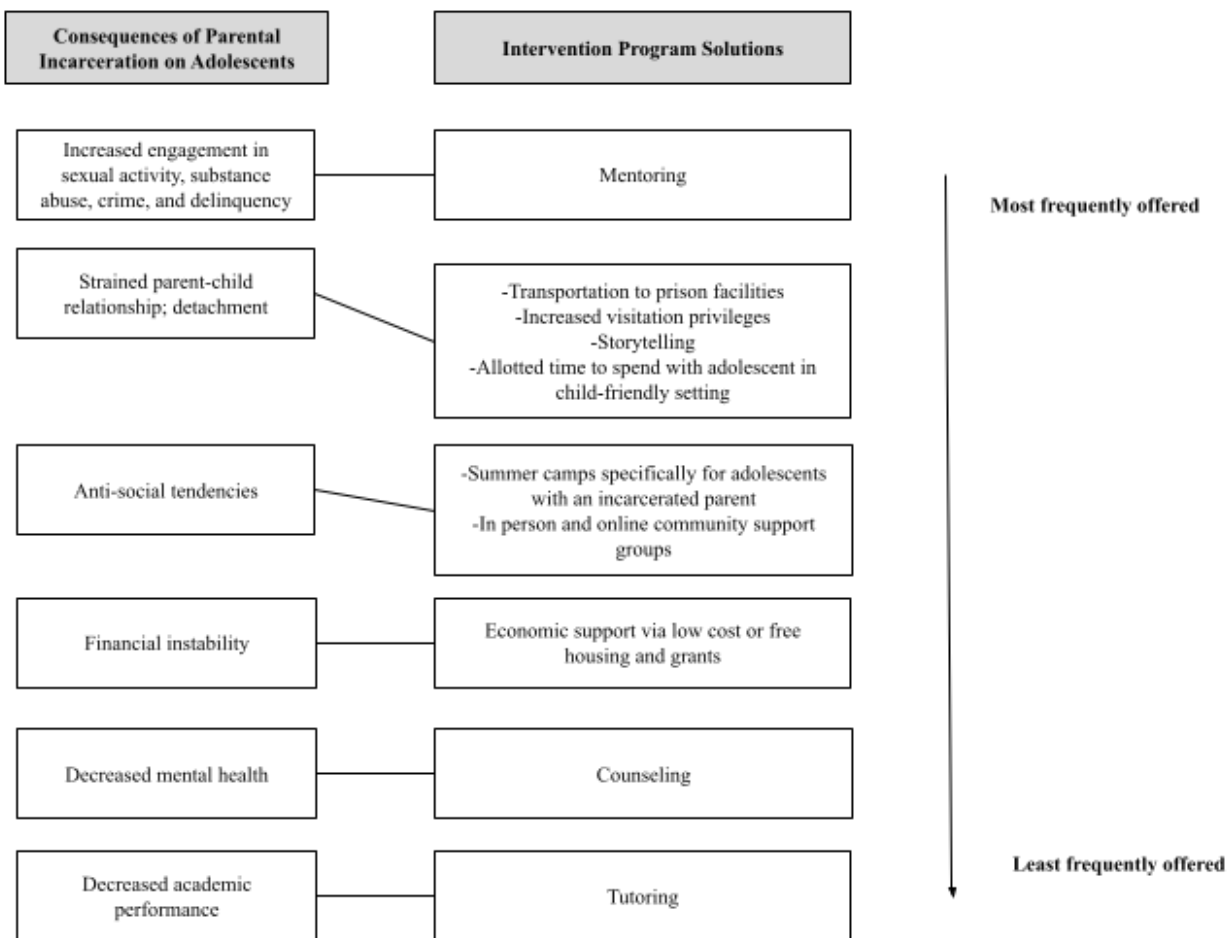


Figure 2. Successful intervention program model for early and middle adolescents based on currently implemented intervention programs.

Big Brother Big Sisters, CHIP (Children of Incarcerated Parents), Girl Scouts Beyond Bars, and Angel Programs at Prison Fellowship were the most notable in-person programs, with the greatest number of branches across the United States. Their success and effectiveness can be attributed to their multi-pronged approach, which targets a significant portion of the effects of parental incarceration, through various activities, events, and services.

Successes from early and middle adolescent intervention programs and developmental distinctions in late adolescents were taken into account to create a hypothetical model for more extensive services offered by organizations. The distinctions in developmental milestones between early/middle and late stages of adolescents were paired with a related

consequence of parental incarceration, based on similarities in behavioral responses between both categories. Interventional solutions were then developed from these behavioral responses, proposing services that would primarily reduce emotional ramifications from consequences of parental incarceration. This model not only emphasizes the continuation and expansion of community support groups and mentoring, but also works towards combating additional, overlooked consequences, such as stigma and the complex parent-teenager/young adult relations, through the inclusion of campaigns and increased opportunities to interact with their parents.

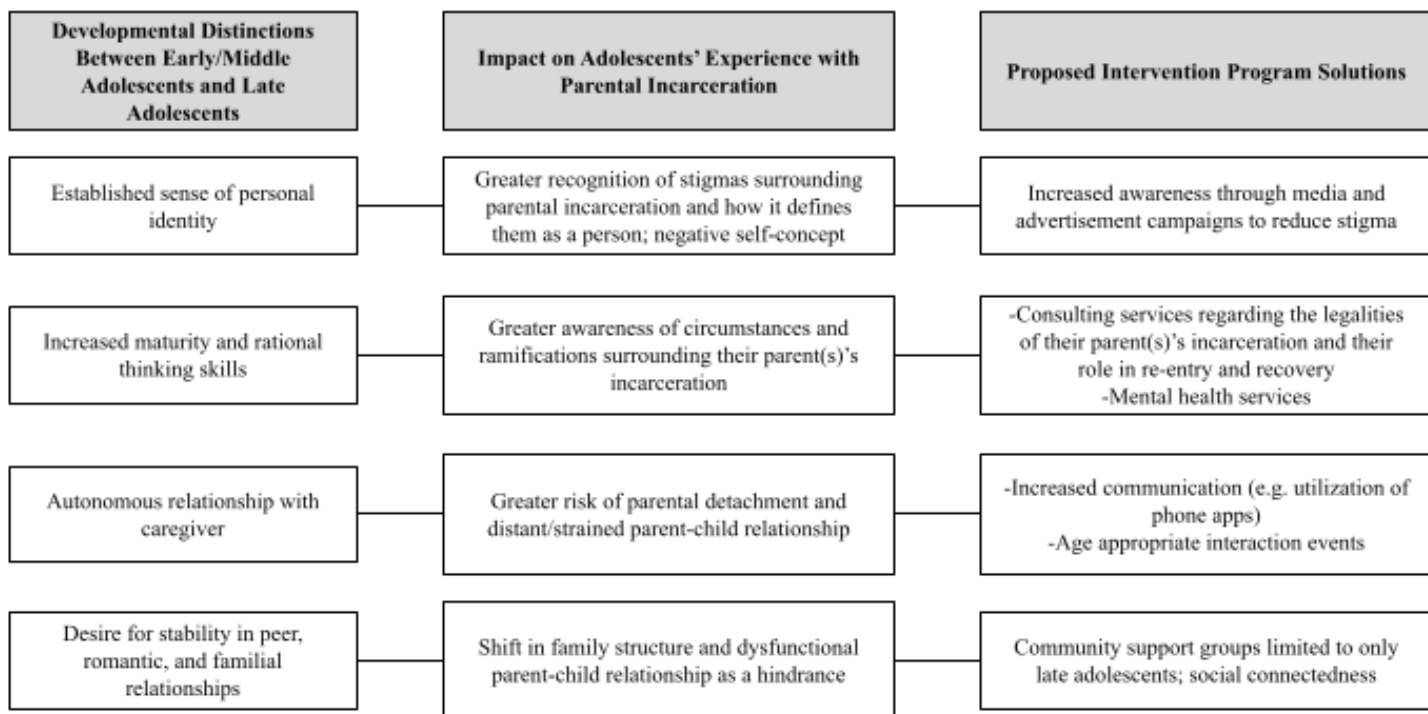


Figure 3. Hypothetical model for intervention program targeted towards late adolescents.

Discussion:

Evidence supporting the scarcity of attention towards late adolescents dealing with parental incarceration is insurmountable in both quantity and quality of offered services, especially in comparison to the wide variety of services available to early, middle, and even pre-adolescent individuals (**Figure 2**). This is a commonality amongst intervention programs across all 50 states and general analyses of available intervention programs (**Figure 1**). Greater attention for late adolescence has been placed on financial funding, through the establishment of scholarship funds (**Table 2**). While this is beneficial, in terms of increasing higher education attainment rates, it only targets one of many consequences. The proposed model in **Figure 3** employs the same multi-pronged approach that late/middle adolescent programs have in order to target multiple ramifications rather than just financial and higher education attainment consequences. Results also suggest that substantial attentiveness is not just limited to early and middle adolescents, but pre-adolescence (ages 5-9) as well. This is

because of beliefs that adolescents and those of such a young age have increased susceptibility to the outlined ramifications, due to their lack of maturity, inability to understand, and easy impressionability. Late adolescents, though facing a different set of challenges due to older age, greater understanding, and developed maturity, still deserve equal recognition. Developmental distinctions, as outlined in **Figure 3**, must be taken into account when producing services for adolescents. Improvements in current and future intervention programs include the inclusion of resources, with separate age-appropriate services, geared towards each stage of adolescence. Nationwide analyses reveal proportional interventional responses, with the availability of programs increasing as the number of reported adolescents with a parent in prison increases (**Table 1**). Because data regarding intervention programs implemented within a penitentiary, rather than an outside organization were not accessible through a public domain, there were limitations on the exact number of intervention programs available. Access to information regarding these programs would

be beneficial in cultivating a more accurate quantification of available programs, as well as provide a greater understanding of nationwide accessibility. Suggestions for future study include (i) the effectiveness of intervention programs upon a parent's release, in comparison to during the period of incarceration, (ii) a psychoanalytical investigation on the timing of a parent's incarceration (i.e. psychological outcomes on younger vs older adolescents), or (iii) an inquiry on the quality and quantity of state specific intervention programs based on prison policies and legislature enacted in that state.

Conclusion:

Adolescents dealing with parental incarceration are already considered an overlooked and understudied population, as per the term "hidden victims". Those within this population between the ages 18-21 are even further overlooked. Misdirected attention to early, middle, and pre-adolescents, though with good intentions, does not take into consideration the lasting impacts of parental incarceration. These effects span far beyond a parent's sentence and well into the young adulthood stage of adolescence, even if the individual was young when the sentencing occurred [3]. Negligence towards the ramifications on late adolescents, who are equally susceptible, is fatal when considering the detriment that parental incarceration can have on an adolescent's life. For late adolescents, limited opportunities for interactions with similarly aged adolescents also dealing with parental incarceration, lack of space for discussion, and overall inadequacy in available resources, further perpetuates isolation, reinforces stigmas, and advances mental health struggles. The sheer nature of parental incarceration, particularly the highly negative outcomes on an adolescent's wellbeing, must catalyze a greater depth in research and funding, as well as garner greater attention towards these

"hidden victims", who evidently, suffer just as much as their incarcerated parents.

References:

- [1] Prison Population by State. (2023). *World Population Review*. <https://worldpopulationreview.com/state-rankings/prison-population-by-state>
- [2] Luk, M., Hui, C., Tsang, S. et al. (2022). Physical and Psychosocial Impacts of Parental Incarceration on Children and Adolescents: A Systematic Review Differentiating Age of Exposure. *Adolescent Research Review*. <https://doi.org/10.1007/s40894-022-00182-9>
- [3] Jones, A., Buntman, F., Ishizawa, H. et al. (2022). The Mental Health Consequences of Parental Incarceration: Evidence from a Nationally Representative Longitudinal Study of Adolescents through Adulthood in the United States. *American Journal of Criminal Justice*. <https://addhealth.cpc.unc.edu/publications/bib/9750/>
- [4] Barrett, D. E. (1996). The Three Stages of Adolescence. *The High School Journal*, 79(4), 333–339. <https://www.jstor.org/stable/40364502>
- [5] Prison Policy Initiative. (2023). New report Mass Incarceration: The Whole Pie 2023 shows that as the pandemic subsides, criminal legal system returning to "business as usual". https://www.prisonpolicy.org/blog/2023/03/14/whole_pie_2023/#:~:text=Although%20prison%20populations%20are%20still,prison%20than%20before%20the%20pandemic
- [6] Bryant, E. (2023). Children Suffer When Parents Are Imprisoned. Vera Institute of Justice. <https://www.vera.org/news/children-suffer-when-parents-are-imprisoned>
- [7] The Annie E. Casey Foundation. Children Who Had a Parent Ever Incarcerated. (2021). *KIDS Count Data Center*. <https://datacenter.aecf.org/data/tables/9688-children-who-had-a-parent-who-was-ever-incarcerated?loc=38&loct=2#detailed/2/2-52/false/2043,1769,1696,1648,1603/any/18927,18928>
- [8] Centers for Disease Control and Prevention. Fast Facts: Preventing Adverse Childhood Experiences. <https://www.cdc.gov/violenceprevention/aces/fastfact.html#:~:text=Adverse%20childhood%20experiences%2C%20or%20ACEs,in%20the%20home%20or%20community>.
- [9] Rutgers University Camden: The National Resource Center on Children and Families of the Incarcerated. Directory of Programs Serving Children

& Families of the Incarcerated. <https://nrccfi.camden.rutgers.edu/resources/directory/>

[10] The University of Minnesota. Understanding Adolescence Seeing Through A Developmental Lens. *State Adolescent Health Resource Center.* <https://sahrc.umn.edu/understanding-adolescence>

Overlapping Alterations in BBB and Inflammation Related Peripheral Targets After Stress or Alcohol Exposure

Sara Mendoza^{1,2}, Lyonna Parise², Scott Russo²

¹USC Brain and Creativity Institute

²Nash Family Department of Neuroscience, Friedman Brain Institute, Icahn School of Medicine at Mount Sinai

Abstract:

Major Depressive Disorder (MDD) and Alcohol Use Disorder (AUD) are comorbid and both exacerbated by stress, suggesting that the two disorders may interface through neuroimmune interactions. One such mechanism could be through dynamic changes in the blood-brain barrier (BBB) as a result of the loss of Claudin-5 (Cldn5), a tight junction protein. Elevations in the concentration of pro-inflammatory cytokines, such as IL-1a, have also been shown to occur in subsets of MDD patients. Thus, Cldn5 increases susceptibility to neuroinflammation by increasing BBB permeability, while an increase in IL-1a mediates the inflammatory response. However, the initial instigator of the peripheral inflammation is unknown. One candidate could be an increase in neutrophil elastase (NE) levels. NE is a proteolytic enzyme that, when oversecreted, is able to 1) degrade Cldn5, and 2) elevate IL-1a levels. In order to investigate the nature of NE's relationship to MDD and AUD, we used mouse models to measure the difference in peripheral effects in response to both stress and alcohol exposure. The peripheral effects that we measured include 1) Cldn5 levels, 2) IL-1a levels, and 3) NE levels. We found that biomarkers of inflammatory response (IL-1a, NE) were elevated after chronic alcohol or stress conditions, but not in acute conditions. All three peripheral effects were elevated when chronic alcohol exposure was combined with acute stress exposure. This suggests that (1) either an increase in neutrophils (neutrophilia) or an oversecretion of NE occurs in chronic alcohol and chronic stress

conditions, and (2) that alcohol and stress have a synergistic effect that involves an interaction between BBB permeability and inflammation.

Introduction:

Major Depressive Disorder (MDD) and Alcohol Use Disorder (AUD) are known to be comorbid. They seem to have a causal linkage, and it was found that the presence of one of these disorders doubles the risk of developing the second disorder [1]. Moreover, stress is a common factor that has been shown to exacerbate both MDD and AUD. Therefore, due to the relationship between stress and immune function, it has been suggested that MDD and AUD interface through neuroimmune interactions stemming from the known immune effects of each disorder [2].

Major breakthroughs have been made regarding the underlying pathophysiology that may contribute to MDD, including findings that suggest the involvement of changes in the blood-brain barrier's (BBB) permeability. In Menard et al. 2017, it was demonstrated using a mouse model that susceptibility to MDD via stress was mediated by down-regulation of the Claudin-5 (Cldn5) protein in response to stress [3]. Cldn5 is a tight junction protein that acts as a gate between blood vessels and the brain, and the stress-induced loss of this protein results in neuroinflammation which causes a heightened susceptibility for depressive-like behaviors. The degradation of Cldn5 at the BBB ultimately results in elevated Cldn5 levels in the blood, because that is where the

protein goes once it is damaged and no longer used at the BBB.

Alcohol is known to insult the BBB by the degradation of tight junction proteins like Cldn5, resulting in increased BBB permeability [4]. The impact of alcohol on the BBB has been further validated in mice models at the level of microvascular endothelial barrier function, which alcohol altered by reorganizing BBB junction proteins [5]. In a study of patients with traumatic brain injury, Cldn5 levels were elevated post-injury, with increased alcohol blood concentration being correlated with increased levels of biomarkers for neuronal damage [6]. These studies ultimately suggest that alcohol impacts BBB permeability through the alteration and damage of Cldn5 proteins.

As a consequence of increased BBB permeability, molecules that are capable of causing neuroinflammation have access to the brain. It was demonstrated that a pro-inflammatory cytokine, IL-6, was permeable in the nucleus accumbens (NAc) of stressed animals, but not in unstressed animals, nor in other brain areas of either stressed or unstressed mice [3]. Additionally, interleukins with roles in the inflammatory response pathway have been shown to be elevated in subsets of MDD patients with inflammatory-related depressions [7]. So, it is clear that Cldn5 loss results in susceptibility to neuroinflammation in the NAc by allowing interleukins to enter the brain and mediate an inflammatory response. However, the exact mechanism behind this damage is unclear, and the initial instigator of the peripheral inflammation is unknown. One potential candidate for this instigator is an elevated concentration of neutrophil elastase (NE), which is a proteolytic enzyme that may be over-secreted as a result of neutrophilia. Interleukin IL-1a is released as part of the inflammatory response signaling pathway, and elevated levels of IL-1a can be attributed to NE over-secretion. Notably, NE was demonstrated to be enzymatically active in

the presence of endothelial cells and is capable of targeting endothelial tight junctions [8][9]. Therefore, elevated NE may offer one explanation for both a loss of Cldn5 as well as elevations of IL-1a.

The present study intends to investigate the impact of alcohol on BBB permeability in response to stress. To do so, we will measure the difference in peripheral effects in response to both acute and chronic stress and alcohol exposure and compare this with the peripheral effects of control animals. The peripheral effects that we will measure include: 1) Cldn5 levels, 2) IL-1a levels, and 3) NE levels.

From this comparison, we anticipate being able to validate the relationship between the effects of alcohol consumption and stress. These results will offer insight into how, mechanistically, NE may be instigating an inflammatory response and/or the degradation of Cldn5.

Materials & Methods:

Animals

Adult male mice were randomly allocated to four experimental groups. Each of the four groups contained an experimental group and a control group. The chronic alcohol group contained 12 wild-type (WT) C57BL/6 mice, with 8 on ethanol (E) and 4 controls with only water (W). The acute alcohol group contained 15 WT C57BL/6, with 10 on ethanol (AE) and 5 controls with only water (AW). The chronic stress group contained 15 C57BL/6 mice, consisting of 5 resilient mice (RES), 5 susceptible mice (SUS), and 5 control mice (CON). The acute stress group contained 15 WT C57BL/6 mice, with 8 experiencing the stress (AS) and 7 unstressed controls (AC). Stress was induced using retired CD1 breeders that were physically aggressive. The stress challenge group contained 16 WT C57BL/6, with 9 on ethanol (E) and 7 on water (W).

Behavioral Testing: Social Interaction

Following chronic stress exposure (**Figure 1**) and acute stress exposure (**Figure 2**), a social interaction test (SI) is performed to determine whether the mice demonstrate a resilient (RES) or susceptible (SUS) phenotype. In the SI, mice from the chronic and acute stress groups are each placed in an arena with an empty box that will serve as the interaction zone. Two trials are conducted for each mouse, the first where the box is empty (no target), and the second where the box contains a random CD1 aggressor that the mouse has not interacted with before (target). The area is delineated to contain an interaction zone (IZ) near the CD1 box. The ratio of time spent in the IZ with target present to target absent determines whether a mouse is resilient or susceptible (to the depression phenotype). Resilient mice (RES) spend more time in IZ when the target is present, whereas susceptible mice (SUS) spend more time in IZ when the target is absent. Social interaction is calculated as the ratio of time spent in the interaction zone with and without a target present. SUS mice have an interaction ratio less than 1 whereas RES mice are above 1.

Stress Paradigm

To induce chronic stress (**Figure 1**), mice experienced the chronic social defeat stress (CSDS) paradigm. Over the course of 10 days, each mouse is paired (daily) with a novel CD1 aggressor for ten minutes, before being moved back to the other side of its cage, where it is separated from the aggressor by a translucent plastic barrier. Mice are not paired with an aggressor if their condition appears critical, and aggressors are re-rotated if they fail to fight the experimental mouse.

To induce acute stress (**Figure 2**), mice were exposed to a subthreshold social stressor (i.e. microdefeat). In this paradigm, each experimental mouse is placed in a cage with a physically aggressive CD1 mouse for five minutes. The mouse is isolated for fifteen minutes before being paired with a new

aggressor, and this cycle repeats until the experimental mouse is defeated by three different aggressor mice. This is a sub-threshold model, so untreated WT mice are not expected to develop a pathological phenotype.

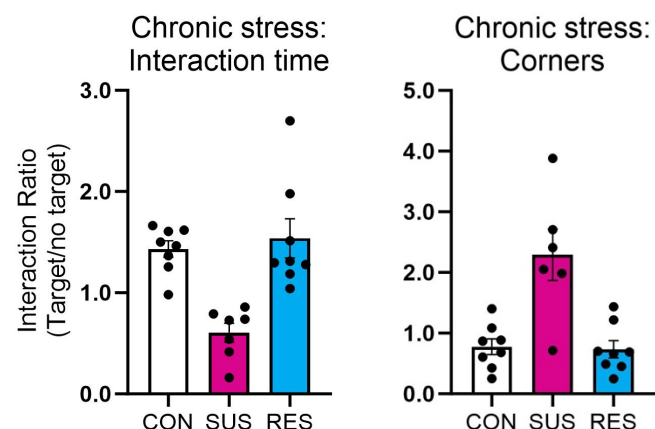
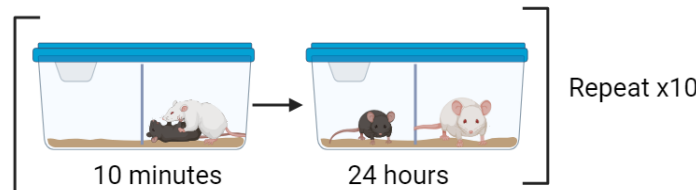


Figure 1. SI on mice that experienced chronic stress. SUS mice interact less with a novel CD1 mouse and spend more time in corners, compared to CON mice or RES mice.

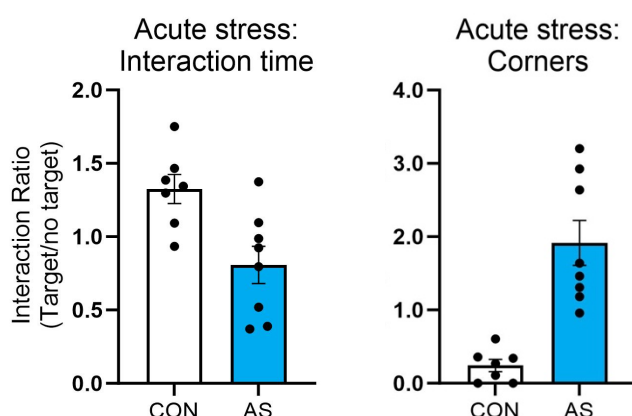
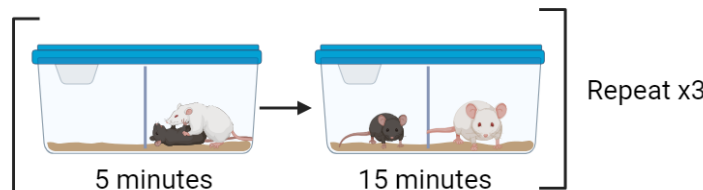


Figure 2. SI on mice that experienced acute stress. Stressed mice (AS) interact less with a novel CD1 mouse and spend more time in corners, compared to control mice (CON).

Alcohol Consumption

A volitional drinking paradigm was used to chronically expose mice to alcohol (**Figure 3**). Specifically, using the intermittent access two-bottle choice paradigm, mice were given one bottle containing water and the other containing 20% ethanol, then after 24 hours given only water for 24 hours. This cycle is repeated Monday – Saturday for 4 weeks. Bottles are weighed each day to calculate the daily consumption of both alcohol and water to determine preference (**Figure 4**). Additional “spill cages” (cages with bottles but no mice) are used to account for water and ethanol lost to drips from moving the bottles.

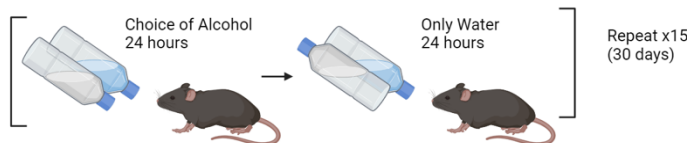


Figure 3. Volitional drinking paradigm for chronic alcohol exposure.

The acute alcohol group was given an acute alcohol exposure, in which they were given one bottle containing water and the other containing 20% ethanol for 24 hours. The mass of the bottles is taken at the end of this period to calculate their consumption and determine preference (**Figure 4**).

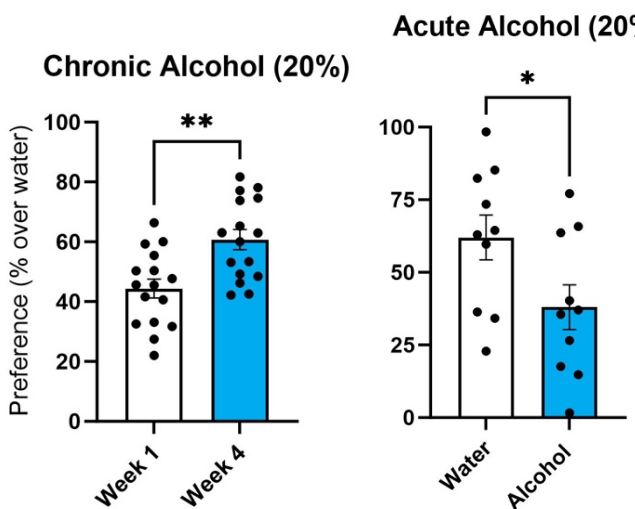


Figure 4. Percent preference of alcohol over water in mice given chronic (24 hours) and acute access to alcohol choice (4 weeks).

Combined Alcohol and Stress

Mice were given 4 weeks of chronic alcohol exposure following the same protocol as the chronic alcohol group. They were then allowed 2 weeks for washout and exposed to a microdefeat. The control group had no alcohol exposure, then experienced a microdefeat. Mice in this group also received behavioral testing following the microdefeat: the SI, elevated plus maze (EPM), and sucrose preference.

Peripheral Marker Assessment: ELISA

Blood samples were collected the day after the SI or after the last alcohol session. Protein assessment was completed using an enzyme-linked immunosorbent assay (ELISA) specific for either neutrophil elastase (NE), IL1a, or claudin 5. All ELISAs were completed according to the manufacturer’s instruction. Briefly, samples were centrifuged and diluted according to the directions specific to each kit and plasma from each group (E, W, AE, AW, RES, SUS, CON, AS, and AC) was assayed and verified against known protein standards (**Figure 5**).

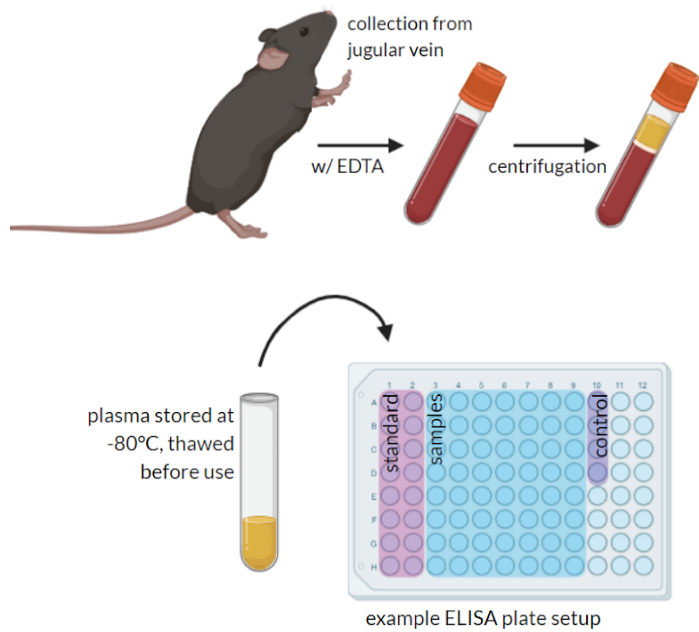


Figure 5. ELISA workflow.

Results:

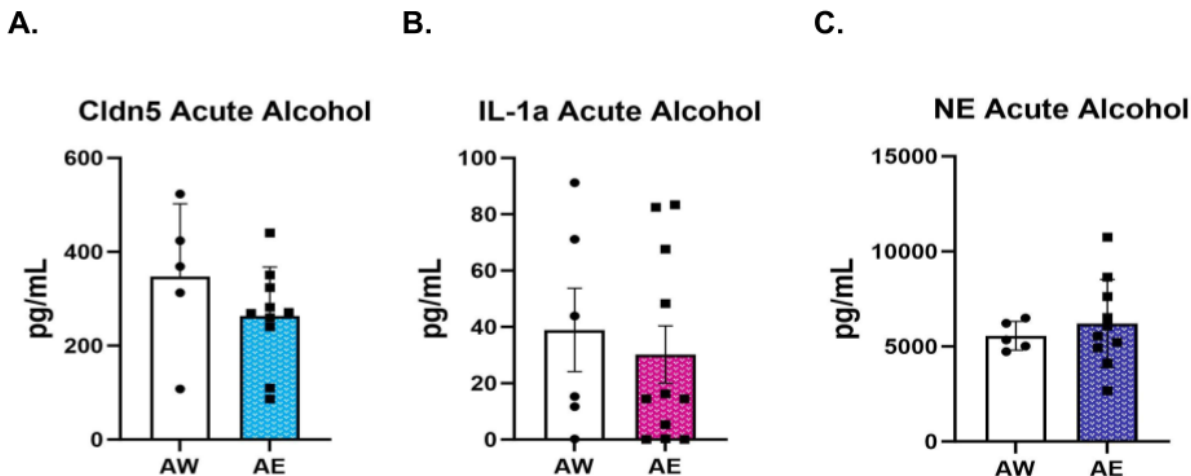


Figure 6. Acute Alcohol ELISAs. (A) Concentrations of Cldn5, (B) IL-1a, and (C) NE in mice that experienced acute alcohol exposure (AE) compared to a control (AW). No significant difference in the concentration of any biomarker was observed.

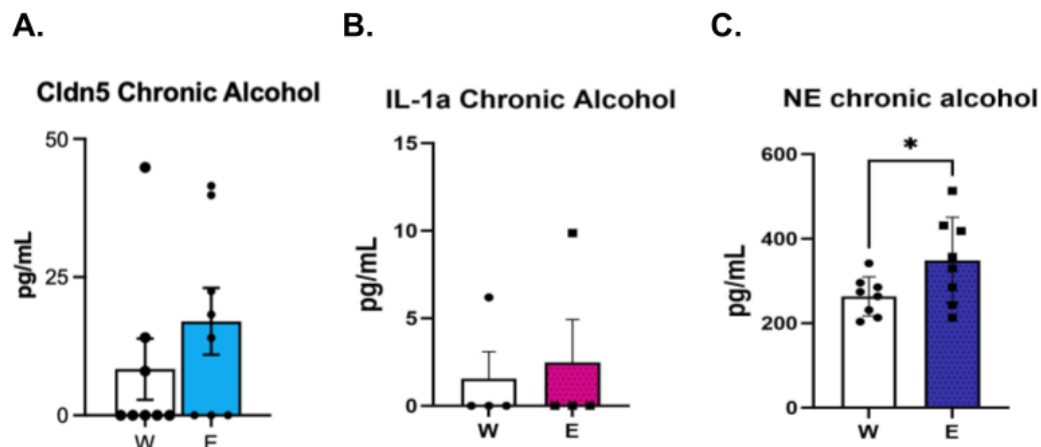


Figure 7. Chronic Alcohol ELISAs. (A) Concentrations of Cldn5, (B) IL-1a, and (C) NE in mice that experienced chronic alcohol exposure (E) compared to a control (W). E were observed to have a higher concentration of NE than W ($p=0.0489$).

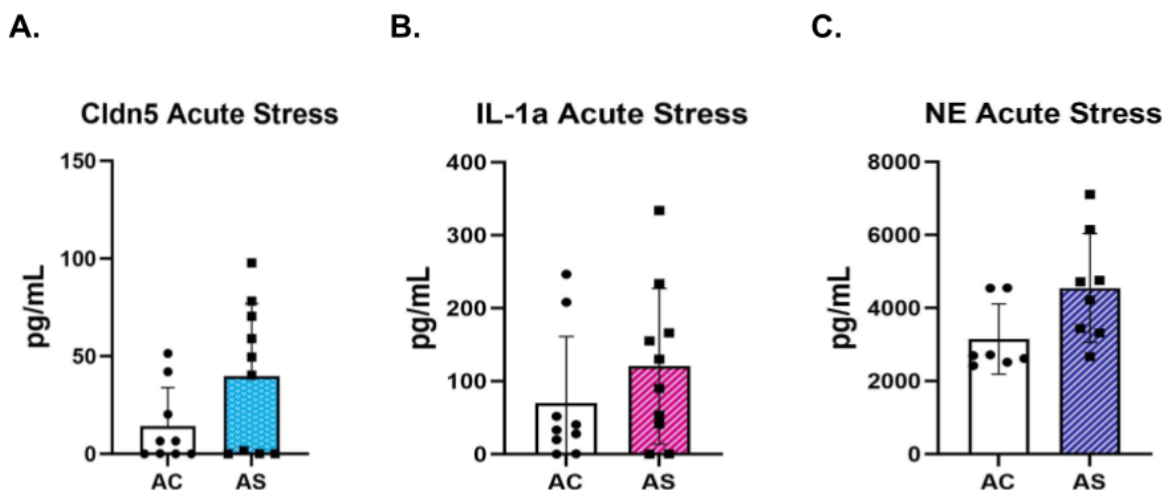


Figure 8. Acute Stress ELISAs. (A) Concentrations of Cldn5, (B) IL-1a, and (C) NE in mice that experienced acute stress (AS) compared to a control (AC). No significant difference in the concentration of any biomarker was observed.

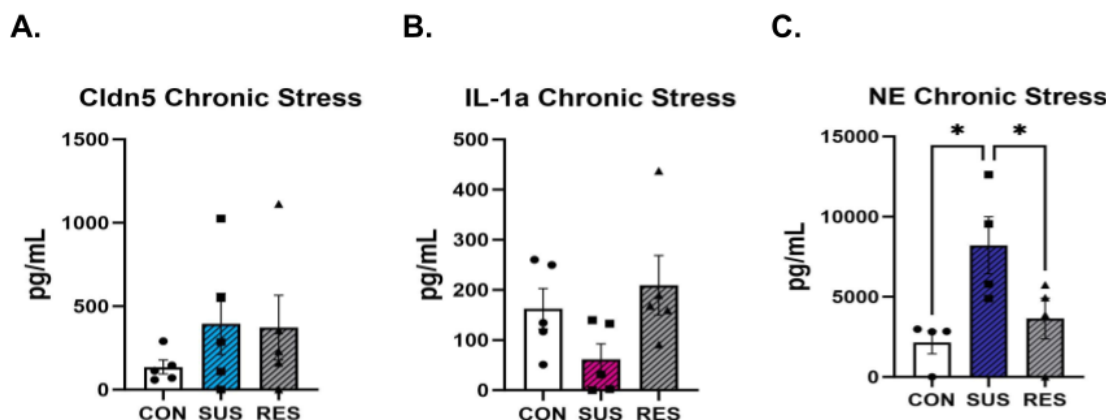


Figure 9. Chronic Stress ELISAs. (A) Concentrations of Cldn5, (B) IL-1a, and (C) NE in mice that experienced chronic stress and demonstrated an avoidance phenotype (SUS) or did not (RES), compared to a control (CON). SUS were observed to have a higher NE concentration compared to both CON and RES ($p = 0.0260$).

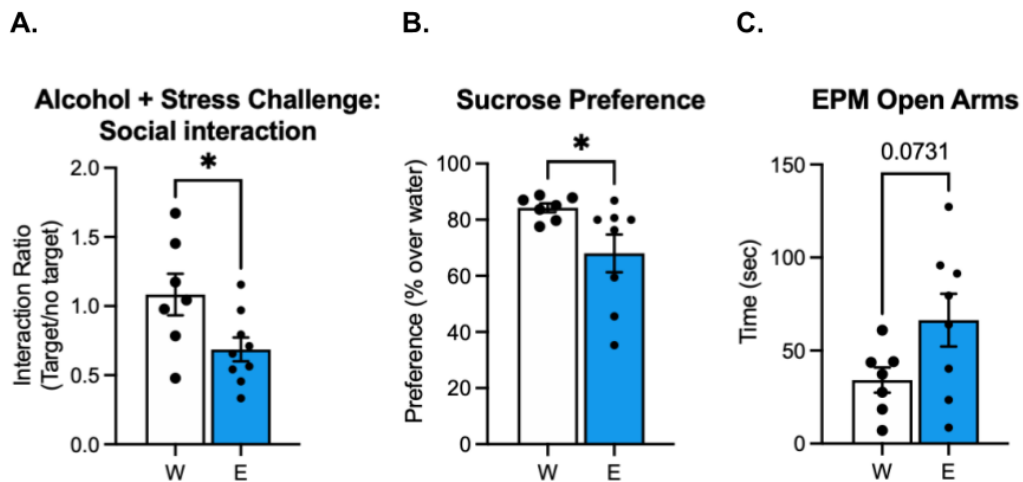


Figure 10. Combined Behavior. Mice previously exposed to ethanol (E) showed decreased interaction time with the target mouse (A, $p=0.007$), a decreased preference for sucrose (B, $p=0.0503$), and more time in the open arms of the EPM (C, $p=0.0731$) compared to mice only given water (W). Both groups experienced acute stress.

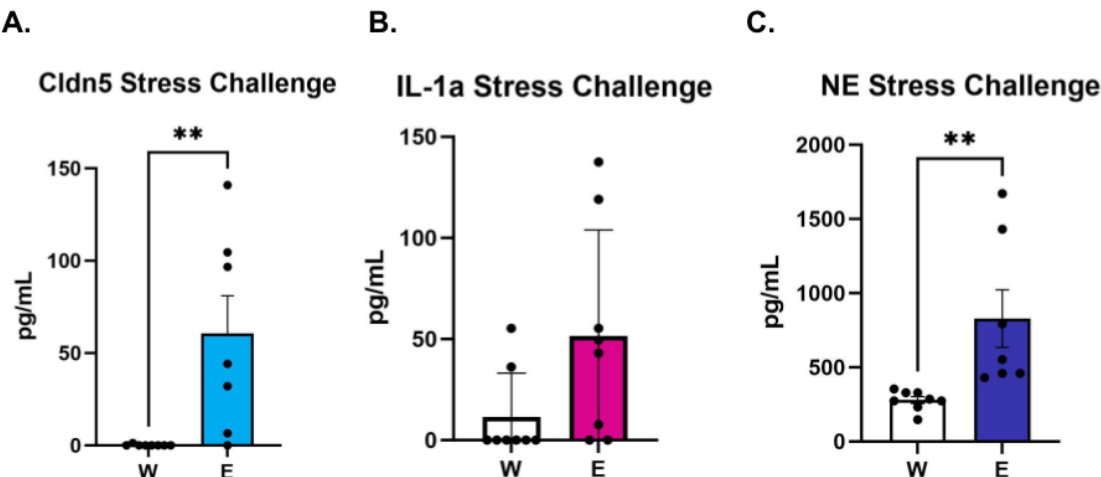


Figure 11. Combined ELISAs. (A) Concentrations of Cldn5, (B) IL-1a, and (C) NE in mice that experienced a chronic alcohol exposure followed by microdefeat (E) compared to a control (W). There was a statistically significant difference observed between the two groups in Cldn5 concentration ($p=0.0070$) and NE concentration ($p=0.0099$). Difference in IL-1a concentration was near significant ($p=0.0660$).

The results from the ELISAs demonstrate that there was no significant difference in Cldn5, IL-1a, or NE after either acute alcohol (**Figure 6**) or acute stress (**Figure 8**). However, there was a significant elevation of NE after chronic alcohol (**Figure 7c**, $p=0.0489$) and chronic stress (**Figure 9c**, $p=0.0260$). There are also non-significant trends demonstrating an increase in Cldn5 after chronic alcohol (**Figure 7a**) and chronic stress (**Figure 9a**), as well as an increase in IL-1a after chronic alcohol (**Figure 7b**). There is also a non-significant trend showing a decrease in IL-1a after chronic stress (**Figure 9b**).

The behavioral results from the combined chronic alcohol and acute stress cohort demonstrates decreased interaction time in the social interaction test (**Figure 10a**, $p=0.007$), a decreased preference for sucrose (**Figure 10b**, $p=0.0503$) and more time spent in the open arms of the EPM (**Figure 10c**, $p=0.0731$) compared to mice who experienced the acute stress without alcohol exposure. The ELISAs from the combined cohort demonstrates they have a strong statistically significant elevation of both Cldn5 (**Figure 11b**, $p=0.0070$) and NE (**Figure 11c**, $p=0.0099$), as well as a near-significant elevation of IL-1a (**Figure 11b**, $p=0.0660$) compared to mice who experienced the acute stress without alcohol exposure.

Discussion:

The concentration of NE is shown to be elevated in both chronic alcohol (**Figure 7c**, $p=0.0489$) and chronic stress (**Figure 9c**, $p=0.0260$) conditions, but not acute alcohol (**Figure 6c**, non-significant) or acute stress (**Figure 8c**, non-significant) conditions. This elevation of NE concentration, especially when combined with trends demonstrating a non-significant increase of Cldn5 in the chronic paradigms (**Figures 7a, 9a**) and a non-significant increase of IL-1a after chronic alcohol (**Figure 7b**), suggests that there is an increase in BBB permeability as well as heightened activity of the inflammatory

response pathway. This suggests that there may be either an increase in the total number of neutrophils (neutrophilia) or there is an oversecretion of NE by existing neutrophils. In either case, the elevation of NE concentration in conjunction with trends in the elevation of Cldn5 and IL-1a concentrations may support the notion that NE could be instigating both a heightened inflammatory response and an increase in BBB permeability (**Figure 12**). Also, because this elevation of NE was only evident in chronic conditions (**Figure 7c, 9c**), this could indicate that it is necessary for the effects of alcohol and stress to accumulate over time in order for NE levels to be impacted. Lastly, NE was elevated after chronic stress in the SUS group compared to both RES and CON groups (**Figure 9c**, $p=0.0260$). Because SUS mice demonstrate the phenotype of depressive-like behaviors and RES do not (despite both experiencing chronic stress), this suggests that NE elevation is specifically related to the development of the depression phenotype,

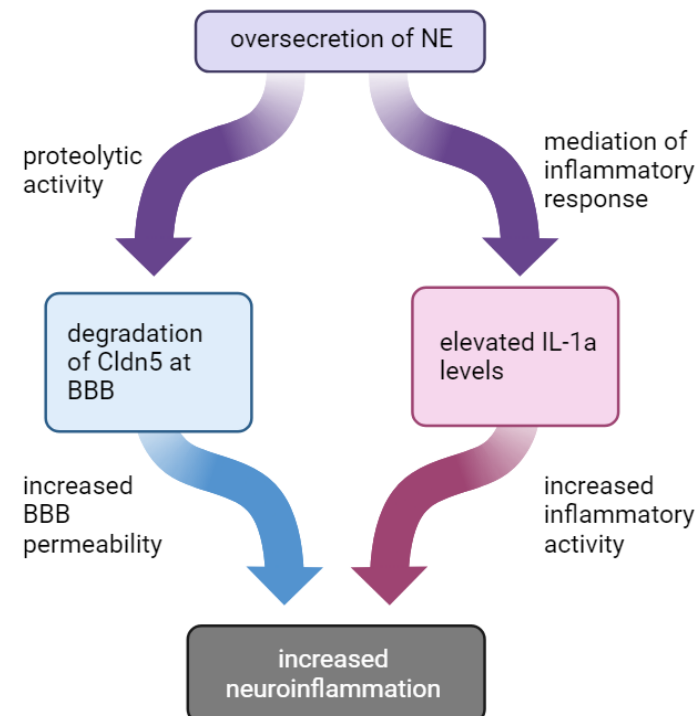


Figure 12. Proposed pathway by which NE instigates an increase in neuroinflammation through both the degradation of Cldn5 at the BBB and the increase in IL-1a via the mediation of the inflammatory response.

rather than only being a response to the chronic stress experience.

The behavior of the combined alcohol and stress challenge group suggests they developed a depression-like phenotype (i.e. demonstrating social avoidance in the SI (**Figure 10a**), anhedonia in sucrose preference (**Figure 10b**), and risk-taking behavior in the EPM (**Figure 10c**)) whereas the group experiencing only the microdefeat did not develop this phenotype. This suggests that the chronic alcohol exposure increased the mice's vulnerability to the development of a depressive-like phenotype following the microdefeat. The ELISA results show that Cldn5 (**Figure 11a**, $p=0.0070$), IL-1a (**Figure 11b**, $p=0.0660$), and NE (**Figure 11c**, $p=0.0099$) are all elevated post-microdefeat in mice that had chronic alcohol exposure, but not those on water. Because these results show a much stronger difference in the biomarker levels compared to any alcohol-alone or stress-alone groups, this suggests there is a synergistic effect between alcohol exposure and stress exposure in the fluctuation of Cldn5, IL-1a, and NE.

One of the major limitations of this study was the absence of behavioral tests for all groups, which would have allowed us to relate the variations in biomarker levels to phenotypical development (i.e. to see whether higher levels of NE correlate with a more dramatic expression of depressive-like behaviors). Another limitation was a lack of brain imaging, which could have confirmed the relationship between elevated Cldn5 blood levels and increased BBB permeability. This has been demonstrated to be true in the literature [3], but this is still a novel biomarker that has not been robustly validated.

To further investigate the role of NE in alcohol and stress, a future study could expose a cohort of NE knockout mice to chronic/acute stress/alcohol exposure in order to determine if NE is necessary to induce the peripheral effects studied here. This could provide insight as to whether NE is the instigator of

the inflammatory action or if there is a separate instigator that elevates the blood concentration of all three biomarkers analyzed in this study. It would also be useful to try microdefeating an acute alcohol group, to further explore the necessity of chronicity in these interactions. Overall, the idea that NE could be both elevating IL-1a levels and degrading Cldn5 at the BBB appears to be a promising mechanism that occurs as a result of alcohol consumption and/or stress.

Conclusion:

By measuring the blood concentration of peripheral biomarkers Cldn5, IL-1a, and NE, we found that chronic exposure to alcohol and chronic stress showed significant elevations in NE, as well as nonsignificant trends in elevations of Cldn5 and IL-1a. This supports the proposed pathway of NE causing both the degradation of Cldn5 at the BBB and the mediation of an inflammatory response via IL-1a, which compound to increase neuroinflammation. However, further study is necessary to confirm this proposal.

The combined alcohol and stress cohort demonstrates a synergistic effect between the two experiences. Although acute stress did not engage peripheral inflammatory mechanisms, when chronic alcohol exposure was followed by a microdefeat, Cldn5 levels were much higher than microdefeated controls (suggesting BBB insult), as well as IL-1a and NE levels (suggesting an inflammatory response). The behavioral results confirm that water exposed mice did not have the same responses, suggesting that the combination of insults more strongly induced phenotypes typical of depression.

References:

- [1] Boden, J.M. and Fergusson, D.M. (2011). Alcohol and depression. *Addiction*, 106: 906-914. <https://doi.org/10.1111/j.1360-0443.2010.03351.x>
- [2] Neupane S. P. (2016). Neuroimmune Interface in the Comorbidity between Alcohol Use Disorder and Major Depression. *Frontiers in immunology*, 7, 655. <https://doi.org/10.3389/fimmu.2016.00655>

[3] Menard, C., Pfau, M. L., Hodes, G. E., Kana, V., Wang, V. X., Bouchard, S., Takahashi, A., Flanigan, M. E., Aleyasin, H., LeClair, K. B., Janssen, W. G., Labonté, B., Parise, E. M., Lorsch, Z. S., Golden, S. A., Heshmati, M., Tamminga, C., Turecki, G., Campbell, M., Fayad, Z. A., ... Russo, S. J. (2017). Social stress induces neurovascular pathology promoting depression. *Nature neuroscience*, 20(12), 1752–1760. <https://doi.org/10.1038/s41593-017-0010-3>

[4] Rubio-Araiz, A., Porcu, F., Pérez-Hernández, M., García-Gutiérrez, M. S., Aracil-Fernández, M. A., Gutierrez-López, M. D., Guerri, C., Manzanares, J., O'Shea, E., & Colado, M. I. (2017). Disruption of blood-brain barrier integrity in postmortem alcoholic brain: preclinical evidence of TLR4 involvement from a binge-like drinking model. *Addiction biology*, 22(4), 1103–1116. <https://doi.org/10.1111/adb.12376>

[5] Alves, N. G., Yuan, S. Y., & Breslin, J. W. (2019). Sphingosine-1-phosphate protects against brain microvascular endothelial junctional protein disorganization and barrier dysfunction caused by alcohol. *Microcirculation*, 26(1), e12506. <https://doi.org/10.1111/micc.12506>

[6] Li, Z., Zhang, J., Halbgieber, S., Chandrasekar, A., Rehman, R., Ludolph, A., Boeckers, T., Huber-Lang, M., Otto, M., Roselli, F., & Heuvel, F. O. (2021). Differential effect of ethanol intoxication on peripheral markers of cerebral injury in murine blunt traumatic brain injury. *Burns & trauma*, 9, tkab027. <https://doi.org/10.1093/burnst/tkab027>

[7] Hodes, G. E., Kana, V., Menard, C., Merad, M., & Russo, S. J. (2015). Neuroimmune mechanisms of depression. *Nature neuroscience*, 18(10), 1386–1393. <https://doi.org/10.1038/nn.4113>

[8] Jerke, U., Hernandez, D. P., Beaudette, P., Korkmaz, B., Dittmar, G., & Kettritz, R. (2015). Neutrophil serine proteases exert proteolytic activity on endothelial cells. *Kidney international*, 88(4), 764–775. <https://doi.org/10.1038/ki.2015.159>

[9] Ushakumari, C. J., Zhou, Q. L., Wang, Y. H., Na, S., Rigor, M. C., Zhou, C. Y., Kroll, M. K., Lin, B. D., & Jiang, Z. Y. (2022). Neutrophil Elastase Increases Vascular Permeability and Leukocyte Transmigration in Cultured Endothelial Cells and Obese Mice. *Cells*, 11(15), 2288. <https://doi.org/10.3390/cells11152288>

The MitoPark Mouse: Mitochondrial Dysfunction and Parkinsonism

Nate Ackerman¹

¹USC Dana and David Dornsife College of Letters, Arts and Sciences

Abstract:

The MitoPark mouse is a preclinical model of Parkinson's disease (PD), an age-related neurodegenerative disorder that targets dopaminergic (DA) neurons in the substantia nigra (SNc) and the nigrostriatal DA system. The model has been used to investigate the role of mitochondrial dysfunction in PD and has supported the hypothesis that severe mitochondrial and respiratory chain dysfunctions can lead to the development of a Parkinsonian phenotype. Knockout of mitochondrial transcription factor A (Tfam) induces severe dysfunction in the respiratory chain of MitoPark mice, which presents progressive motor and nonmotor symptoms of PD at age 14-15 weeks—strikingly similar to the adult-age onset and symptomatic profile of PD in humans. Levodopa therapy, the primary treatment for PD, initially ameliorates symptoms but eventually causes both MitoPark mice and humans to develop dyskinesias. These similarities suggest that the MitoPark mouse is a utile model for investigating the pathophysiology of Parkinsonism and efficacy of therapeutics in preclinical study within the scope of addressing and understanding mitochondrial dysfunction in PD.

Introduction:

Parkinson's disease (PD) is the second most common neurodegenerative disorder, with over six million cases worldwide. The disease's pathophysiology is characterized by the progressive degeneration of dopaminergic (DA) neurons in the substantia nigra pars compacta (SNc), resulting in adult age onset of motor and cognitive symptoms [1]. Despite its worldwide burden and extensive research efforts, there are no preventative or disease-

altering treatments which halt PD's progression, and its exact cause is unknown, with 85% of cases arising sporadically [2]. However, postmortem analysis of PD patients' brains has revealed an increase in respiratory-chain deficient DA neurons and significantly reduced expression of mitochondrial transcription factor A (Tfam), which supports the assertion that mitochondrial dysfunction is heavily implicated in the pathogenesis of PD, thereby providing a potential therapeutic target [3, 4].

In this review, we collate information from past research conducted using the MitoPark mouse, including its recombinant construction procedure, pathophysiological validity and rationale, past research findings, experimentally-uncovered limitations, and proposed future research with the model. The MitoPark mouse is a preclinical model which selectively knocks out Tfam in DA neurons, generating a Parkinsonian phenotype of progressive SNc degeneration with worsening adult-age onset motor and cognitive defects [5]. Additional Parkinsonian features arise as a result of Tfam knockout, including gastrointestinal dysfunction, oxidative stress, and inflammation [6, 7]. Thus, the MitoPark mouse model has utility in investigating the efficacy of PD therapeutics in the scope of mitochondrial dysfunction. In the first paper describing the model, MitoPark mice treated with levodopa responded similarly to humans and experienced improvements in motor and cognitive function, but eventually became hypersensitized to the treatment [8, 9]. Furthermore, the MitoPark mouse alone and its response to levodopa can be used as negative and positive controls, respectively, for studying novel therapeutics. However,

some therapeutics are incompatible with this model.

While many pathologies of PD are conserved in the MitoPark mouse, α-synuclein-containing Lewy bodies are not, limiting research into therapeutics that target this protein [5]. In addition, Tfam polymorphisms are not directly linked to PD, and Tfam expression is not completely knocked out in human PD; therefore the MitoPark mouse model's narrow focus on mitochondrial dysfunction oversimplifies PD's true complexity in humans. Furthermore, the MitoPark mouse model is simplistic in that Tfam knockout is the only etiological factor and does not account for the broad spectrum of genetic and environmental factors that human PD encapsulates. Despite these limitations, the MitoPark mouse model has been utilized by researchers seeking to investigate various therapies' mechanisms of action and effect on a cellular level for treatment of PD and levodopa dyskinesia.

Construction of the MitoPark Mouse:

The MitoPark mouse is created using Cre-Lox recombination to specifically target DAT promoter expressing tissues: the SNc and VTA. First, DAT-cre mice are created by introducing *cre* and neomycin into the DAT locus, then excising neomycin [5]. DAT-*cre* mice can then be crossed with Tfam^{loxP} mice via *cre*-recombinase activity, producing the MitoPark mouse. The genetic recombination approach to making the MitoPark mouse gives it an advantage over toxin-based models such as MPTP or Reserpine, as the MitoPark is both non-pleiotropic and progressive, as opposed to the acute nature of many toxin models.

Background Information Supporting the Validity of MitoPark Mice:

MitoPark mice's mitochondrial transcription factor A (Tfam) is selectively knocked out in neurons which express the DA transporter (DAT) promoter. The Tfam protein is essential for mitochondrial DNA

(mtDNA) transcription initiation and regulation, so Tfam knockout causes mtDNA depletion and suppression, resulting in mitochondrial respiratory chain dysfunction as well as impaired mitochondrial biogenesis [7]. Decreased Tfam expression has been implicated in human PD, supporting the utilization of induced mitochondrial dysfunction via Tfam knockout in MitoPark mice [4,7]

The DAT-expressing tissues targeted for Tfam knockout most notably include the SNc and the ventral tegmental area (VTA). In human PD, degeneration first occurs in the SNc, followed by the VTA during late-stage PD; this sequencing is conserved in the MitoPark mouse [5]. These structures produce dopamine, a neurotransmitter responsible for movement, reward, pleasure, and other processes. Progressive degeneration of the SNc and VTA leads to decreased DA production and neurotransmission. Over time, this leads to the development of motor symptoms such as tremor, rigidity, and bradykinesia as well as cognitive symptoms such as dementia and depression [1]. Similar to PD in humans, the MitoPark model displays progressive development of Parkinsonian symptoms, both motor and nonmotor [5].

MitoPark mice display outwardly normal phenotypes until the age of 12 weeks, whereupon degeneration of DA innervations in the nigrostriatal pathway appear in tissue samples. In addition, severely reduced mtDNA expression and cytoplasmic aggregates, while asymptomatic, are detected as early as 6 weeks of age. At 14-15 weeks, the mice display reduced locomotion and exploratory behavior. These symptoms progressively worsen, and at 20 weeks the mice displayed outward Parkinsonian locomotor phenotypes and high concentrations of DA metabolites DOPAC and HVA in the striatum, indicating DA deficiency. At 45 weeks of age, the mice's condition became exceedingly poor, warranting euthanization [5]. This

progressive timeline allows for a longitudinal analysis of DA concentration, SNC/VTA degeneration, and motor/nonmotor symptoms.

Levodopa (L-DOPA) is the blood-brain barrier permeable precursor to DA and has been the primary treatment for PD since the 1960s. It provides temporary relief of motor symptoms by replenishing the DA depleted from SNC degeneration, thereby restoring nigrostriatal neurotransmission and even making dramatic improvements in patient quality of life. However, L-DOPA therapy is not a disease-modifying therapeutic, and as PD progresses, the efficacy threshold increases and the dyskinesia threshold decreases, increasing the likelihood of adverse effects, most notably dyskinesia and motor fluctuations. These responses to L-DOPA occur because glutamatergic receptors are changed as a result of high levels of DA stimulation [10].

Past Versatility of MitoPark Mice in Therapeutic Studies:

While the MitoPark mouse has not elucidated any disease-halting or curative therapies, numerous ameliorative approaches have been studied using the model. MitoPark models have demonstrated the efficacy (and oftentimes inefficacy) of mitochondrial dysfunction-targeting therapies ranging from novel pharmaceuticals, exercise, probiotics, and antioxidants on the treatment and delaying of Parkinsonism and levodopa-carbidopa related dyskineticas.

PT320, an anti-dyskinetic drug and novel pharmaceutical, completed Phase 2 clinical trials in April 2021. In addition to being studied in humans, PT320 was studied preclinically with the MitoPark mouse model. When administered before the onset of dyskinesia in MitoPark mice, the drug was found to significantly reduce the severity of involuntary dyskinetic movements and encourage the neurotransmission of DA in the nigrostriatal tract [11].

The MitoPark mouse has also been used as a model for exploring the effects of exercise on motor ability, oxidative phosphorylation, DA levels. MitoPark mice who exercised on a wheel were found to perform significantly better on rotarod and beam walking tests compared to non-exercised mice [12]. PET and HPLC assays revealed that exercised mice also favored ATP production via oxidative phosphorylation rather than glycolysis and had slightly increased levels of DA compared to non-exercised mice [12].

The mechanism of action and ameliorative effects of quercetin, an over-the-counter antioxidant, were also studied using MitoPark mice. Quercetin was found to activate cell-survival kinases, which upregulate PGC-1 α and Tfam, stimulating mitochondrial biogenesis and neuroprotection. The relief of oxidative stress and mitochondrial dysfunction provided by quercetin resulted in reversal of striatal DA depletion, improved behavioral and motor symptoms, and reduced TH neuron death [13].

Gastrointestinal dysfunction is a common symptom of early PD that is implicated in the progression of PD, both in humans and MitoPark mice, but is often overlooked as a potential therapeutic target [6]. The administration of daily probiotics to MitoPark mice demonstrated significant improvements in motor function and preserved TH-stained DA neurons in the SNC from degeneration, highlighting the clinical potential for probiotics in slowing neurodegeneration [14].

Limitations of the MitoPark Mouse:

The MitoPark mouse, although faithful to human PD in its progressive nature, development of various Parkinsonian motor and nonmotor symptoms, and positive to dyskinetic levodopa response, has several validity-reducing limitations to consider.

Genetic knockout of Tfam gives rise to many limitations for the model; there is “no

data showing a TFAM polymorphism in Parkinson's disease," so the MitoPark mouse can provide little insight into familial forms of PD unless additional genetic modifications are introduced [15]. In addition, while Tfam levels are reduced in PD patients, the gene is not completely knocked out. Thus, the role of Tfam in the MitoPark mouse is inflated and utilizes a powerfully simplified, one-punch etiology for mitochondrial dysfunction and PD while, in reality, the disease is incredibly complex and is a result of many compounding factors. Furthermore, the selectivity of Tfam knockout to DAT-expressing tissues limits the model, as many other tissues are affected in human PD.

The lack of significant sexual dimorphism in the brains of MitoPark mice also limits researchers studying sex-based differences in PD [16]. Another species-specific limitation is the narrow range of behavioral and non-motor symptoms, which also have questionable translatability to humans. Therefore, it is possible that therapeutics' adverse effects that did not present in MitoPark mice may present in humans.

A major limitation described in the MitoPark mouse's debut paper is the lack of α -synuclein Lewy bodies, a common pathological feature of PD. This indicates that the MitoPark phenotype develops independently of α -synuclein, limiting research into drugs which target the protein, such as Rapamycin, and research into the origin and role of Lewy bodies throughout PD's progression [5].

Future Directions and Improvements:

Crossing MitoPark mice with an α -synuclein strain of mouse may encourage Lewy body formation, which could create additional research avenues and create a model which more closely resembles human PD. In addition, other genetic or environmental factors can be incorporated to more closely resemble the human experience of PD.

Microplastics pose a potential threat to public health, as the ingestion of these and other "forever chemicals" has unknown age-related effects. The introduction of microplastics into the MitoPark mouse's diet could provide insight into their possible implications in PD and alert consumers as to which products to avoid. Similarly, blue-light studies whereupon mice are exposed to an iPhone screen for 6 hours a day could mimic the average human's daily life experience and possibly be revealed as an accelerating factor in PD progression.

Antioxidants and other drugs related to oxidative stress and mitochondrial dysfunction are suited for study with the MitoPark mouse model. Cocktails of pharmaceuticals, probiotics, levodopa-carbidopa, other supplements and therapies such as exercise could be created to study potential overlapping benefits. For example, probiotic and quercetin supplementation paired with daily exercise could provide low-cost benefits which may be translated in clinical studies.

Neuroprotective agents such as growth hormone, which is permeable to the blood brain barrier, could be tested as a possible therapeutic. Injecting an artery known to supply the SNC with oxygen with small quantities of the hormone could potentially induce a neuroprotective effect and stimulate neuronal growth. This would theoretically slow the progression of PD and potentially temporarily reverse the effects of neurodegeneration, but would not resolve the cause of mitochondrial dysfunction, Tfam knockout. Instead, attempts could be made using the CRISPR-Cas9 to repair the Tfam gene to partial functionality in hopes of reducing mitochondrial dysfunction and PD progression.

Conclusion:

PD is a progressive neurodegenerative disorder characterized by degeneration of DA neurons in the SNC, resulting in motor symptoms such as bradykinesia and rigidity

as well as nonmotor symptoms such as dementia and sleep disturbances. After decades of research, the leading treatment for PD remains levodopa therapy, which is known to only delay the disease's progression and eventually cause dyskinetic motor symptoms as a result of glutamatergic receptor sensitization to DA. Despite its severe side effects, the consensus in the scientific community remains that it is the most effective option, as discovery of disease-altering therapeutics has eluded researchers [11]. However, mouse models like MitoPark allow inchwise progress to be made towards elucidating the pathophysiology of PD and finding a more effective, progression-halting treatment for the disease. Regrettably, investing large amounts of money into drug discovery in hopes of finding a drug superior to levodopa is likely to yield diminishing returns with our current understanding of the disease.

The MitoPark mouse is ultimately a model of mitochondrial dysfunction that happens to create a Parkinsonian phenotype. Dr. Mats Ekstrand, the inventor of the MitoPark mouse, has stated that his intention was to create a model that supports the hypothesis that mitochondrial dysfunction alone can result in a progressive Parkinsonian phenotype [17]. The selective knockout of Tfam in DAT expressing neurons via Cre-LoxP recombination results in adult-age onset motor and nonmotor symptoms accompanied by PD's hallmark SNC degeneration. In addition, the MitoPark mouse also experiences a positive initial response to levodopa therapy, but eventually becomes dyskinetic, similarly to humans undergoing treatment with the drug [5]. Because of its response to levodopa, the preclinical MitoPark model is suitable for studying the potential efficacy of novel anti-dyskinetic therapeutics such as PT320 before investing more money into human clinical trials [11].

While the MitoPark model does not produce a-synuclein Lewy bodies and its

etiological cause of Parkinsonism is a genetic knockout of Tfam that does not occur in humans, its progressive nature makes utilize it for conducting longitudinal studies into the progression of a PD-like phenotype. In addition, mitochondrial dysfunction has been implicated in PD, making its isolation as the sole etiological cause in MitoPark mice useful for separating the role of mitochondrial dysfunction from environmental and genetic causes of the disease. At various points throughout longitudinal studies, MitoPark mice can be sacrificed and tissue samples can be collected to shed light on the effect of severe respiratory dysfunction within the SNC and VTA on the mouse's physiology, as well as the mechanism, effects, and possible efficacy of a wide range of PD therapeutics that can assist in symptom management and delaying of disease progression.

References:

- [1] Zhong, Q.-Q., & Zhu, F. (2022). Trends in prevalence cases and disability-adjusted life-years of parkinson's disease: Findings from the global burden of disease study 2019. *Neuroepidemiology*, 56(4), 261-270. <https://doi.org/10.1159/000524208>
- [2] Tran, J., Anastacio, H., & Bardy, C. (2020). Genetic predispositions of parkinson's disease revealed in patient-derived brain cells. *Npj Parkinson's Disease*, 6(1). <https://doi.org/10.1038/s41531-020-0110-8>
- [3] Bender A, Krishnan KJ, Morris CM, Taylor GA, Reeve AK, Perry RH, Jaros E, Hersheson JS, Betts J, Klopstock T, et al. (2006) *Nat Genet* 38:515–517
- [4] Chen, C., Vincent, A. E., Blain, A. P., Smith, A. L., Turnbull, D. M., & Reeve, A. K. (2020). Investigation of mitochondrial biogenesis defects in single substantia nigra neurons using post-mortem human tissues. *Neurobiology of Disease*, 134, 104631. <https://doi.org/10.1016/j.nbd.2019.104631>
- [5] Ekstrand, M. I., Terzioglu, M., Galter, D., Zhu, S., Hofstetter, C., Lindqvist, E., Thams, S., Bergstrand, A., Hansson, F. S., Trifunovic, A., Hoffer, B., Cullheim, S., Mohammed, A. H., Olson, L., & Larsson, N.-G. (2007). Progressive parkinsonism in mice with respiratory-chain-deficient dopamine neurons. *Proceedings of the National Academy of Sciences*, 104(4), 1325-1330. <https://doi.org/10.1073/pnas.0605208103>

- [6]** Ghaisas, S., Langley, M. R., Palanisamy, B. N., Dutta, S., Narayanaswamy, K., Plummer, P. J., Sarkar, S., Ay, M., Jin, H., Anantharam, V., Kanthasamy, A., & Kanthasamy, A. G. (2019). MitoPark transgenic mouse model recapitulates the gastrointestinal dysfunction and gut-microbiome changes of Parkinson's disease. *Neurotoxicology*, 75, 186–199. <https://doi.org/10.1016/j.neuro.2019.09.004>
- [7]** Sterky, F. H., Lee, S., Wibom, R., Olson, L., & Larsson, N.-G. (2011). Impaired mitochondrial transport and parkin-independent degeneration of respiratory chain-deficient dopamine neurons in vivo. *Proceedings of the National Academy of Sciences*, 108(31), 12937-12942. <https://doi.org/10.1073/pnas.1103295108>
- [8]** Galter, D., Pernold, K., Yoshitake, T., Lindqvist, E., Hoffer, B., Kehr, J., Larsson, N.-G., & Olson, L. (2010). MitoPark mice mirror the slow progression of key symptoms and l-dopa response in parkinson's disease. *Genes, Brain and Behavior*, 9(2), 173-181. <https://doi.org/10.1111/j.1601-183X.2009.00542.x>
- [9]** Gellhaar, S., Marcellino, D., Abrams, M. B., & Galter, D. (2015). Chronic l-DOPA induces hyperactivity, normalization of gait and dyskinetic behavior in MitoPark mice. *Genes, Brain and Behavior*, 14(3), 260-270. <https://doi.org/10.1111/gbb.12210>
- [10]** Stocchi, F. (2003). Prevention and treatment of motor fluctuations. *Parkinsonism & Related Disorders*, 9, 73-81. [https://doi.org/10.1016/S1353-8020\(03\)00021-X](https://doi.org/10.1016/S1353-8020(03)00021-X)
- [11]** Kuo, T.-T., Chen, Y.-H., Wang, V., Huang, E. Y.-K., Ma, K.-H., Greig, N. H., Jung, J., Choi, H.-I., Olson, L., Hoffer, B. J., & Tseng, K.-Y. (2023). PT320, a sustained-release glp-1 receptor agonist, ameliorates l-dopa-induced dyskinesia in a mouse model of parkinson's disease. *International Journal of Molecular Sciences*, 24(5), 4687. <https://doi.org/10.3390%2Fijms24054687>
- [12]** Lai, J.-H., Chen, K.-Y., Wu, J. C.-C., Olson, L., Brené, S., Huang, C.-Z., Chen, Y.-H., Kang, S.-J., Ma, K.-H., Hoffer, B. J., Hsieh, T.-H., & Chiang, Y.-H. (2019). Voluntary exercise delays progressive deterioration of markers of metabolism and behavior in a mouse model of parkinson's disease. *Brain Research*, 1720, 146301. <https://doi.org/10.1016/j.brainres.2019.146301>
- [13]** Ay, M., Luo, J., Langley, M., Jin, H., Anantharam, V., Kanthasamy, A., & Kanthasamy, A. G. (2017). Molecular mechanisms underlying protective effects of quercetin against mitochondrial dysfunction and progressive dopaminergic neurodegeneration in cell culture and mitopark transgenic mouse models of parkinson's disease. *Journal of Neurochemistry*, 141(5), 766-782. <https://doi.org/10.1111/jnc.14033>
- [14]** Hsieh, T.-H., Kuo, C.-W., Hsieh, K.-H., Shieh, M.-J., Peng, C.-W., Chen, Y.-C., Chang, Y.-L., Huang, Y.-Z., Chen, C.-C., Chang, P.-K., Chen, K.-Y., & Chen, H.-Y. (2020). Probiotics alleviate the progressive deterioration of motor functions in a mouse model of parkinson's disease. *Brain Sciences*, 10(4), 206. <https://doi.org/10.3390/brainsci10040206>
- [15]** Zhang, Y., Granholm, A.-C., Huh, K., Shan, L., Diaz-ruiz, O., Malik, N., Olson, L., Hoffer, B. J., Lupica, C. R., Hoffman, A. F., & Backman, C. M. (2012). PTEN deletion enhances survival, neurite outgrowth and function of dopamine neuron grafts to mitopark mice. *Brain*, 135(9), 2736-2749. <https://doi.org/10.1093/brain/aws196>
- [16]** Spring, S., Lerch, J. P., & Henkelman, R. M. (2007). Sexual dimorphism revealed in the structure of the mouse brain using three-dimensional magnetic resonance imaging. *NeuroImage*, 35(4), 1424-1433. <https://doi.org/10.1016/j.neuroimage.2007.02.023>
- [17]** Ekstrand, M. I., & Galter, D. (2009). The MitoPark Mouse - an animal model of Parkinson's disease with impaired respiratory chain function in dopamine neurons. *Parkinsonism & related disorders*, 15 Suppl 3, S185–S188. [https://doi.org/10.1016/S1353-8020\(09\)70811-9](https://doi.org/10.1016/S1353-8020(09)70811-9)

Effect of *Chd8* haploinsufficiency on cerebellar volume and social dominance in B6-CC17 and B6-CC61 mouse strains

Khalifa Elmagarmid¹, Manal Tabbaa², Pat Levitt²

¹USC Dana and David Dornsife College of Letters, Arts and Sciences

²The Saban Research Institute, Children's Hospital Los Angeles

Abstract:

Although the cerebellum has long been noted to control motor behavior, recent literature shows that the cerebellum also regulates social behavior in mice through interactions with other brain regions like the ventral tegmental area [1]. Therefore, we hypothesized that the cerebellum was impacted in mice with altered social behaviors due to mutations in the high-confidence autism risk gene, Chromodomain Helicase DNA Binding protein 8 (CHD8). The objective of this study was to utilize a mouse genetic reference panel (GRP) to investigate the relationship between cerebellar volumes in Chd8 heterozygous (Chd8+/-) male and female mice with differential susceptibility to abnormal social behaviors compared to typical wild-type (WT) mice. The Collaborative Cross (CC) GRP was derived from eight founders and creates a genetically linked cohort to demonstrate systematically the role of genetic background on ASD-related traits. Differences in cerebellum volume were quantified after in-vivo MRI scans on 99 subjects from two GRP strains that showed differences in susceptibility to social dominance due to Chd8 haploinsufficiency. Analysis of the cerebellum volume revealed the presence of a Chd8 genotype effect for enlarged cerebellar volumes, especially within B6-CC61 females, which displayed social dominance over wild-type counterparts.

Introduction:

Autism Spectrum Disorder (ASD) is a neurodevelopmental disorder that manifests itself with a broad range of symptoms, the most notable being difficulty with social interactions. Symptoms include macrocephaly, sleeping disorders, gastrointestinal issues, and mood disorders all of which impair the individual's quality of life. Regarding the spectrum, certain individuals with ASD may be nonverbal while others are indistinguishable from their neurotypical peers [2]. Additionally, certain individuals may require assistance with daily activities such as wearing clothes while others are completely independent. The physical health of an individual with ASD is intertwined with the financial costs which can prevent families from providing the best standard of care. The lifetime cost for an individual without a co-occurring intellectual disability is approximately \$1.4 million while for those with an intellectual disability, it's \$2.4 million. On a broader scale, the costs of ASD will grow from USD 268 billion in 2015 to USD 461 billion in 2025 when accounting for the loss of parent working days, educational support, and special health services which is a testament to the growing population [3].

While the etiology of autism is not yet fully understood, researchers have identified that loss of function mutations in the chromodomain helicase DNA-binding protein 8 (*CHD8*) gene are highly penetrant for ASD and macrocephaly [4], [5], [6]. This gene encodes a protein that is a transcription factor and regulates chromatin remodeling

consequently altering the extent to which DNA is packed. Homozygous *CHD8* loss of function mutations are paramount to survival and lead to fatal embryos. In the clinical population, individuals with heterozygous loss of function in *CHD8* on one allele have a high prevalence of Autism (87%) and macrocephaly (80%) in addition to intellectual disability, gastrointestinal disturbances, and anxiety, with variable penetrance and severity [4].

A critical challenge in neurodevelopmental disorder (NDD) research is the clinical heterogeneity that arises despite common genetic mutations. Research has implicated that genetic

background contributes to these differences [7], [8]. However, basic research into underlying mechanisms largely uses single inbred strains which is the same thing as studying one genetic background. The use of inbred strains in preclinical and *in vivo* research offers genetic reproducibility given that the same genotype can be reproduced for each subject across labs and experiments. However, using a single inbred strain does not elucidate the effect of diverse genetic backgrounds on the manifestation of trait disruptions due to genetic risk factors. To show the impact of genetic background on trait disruptions due to *Chd8*

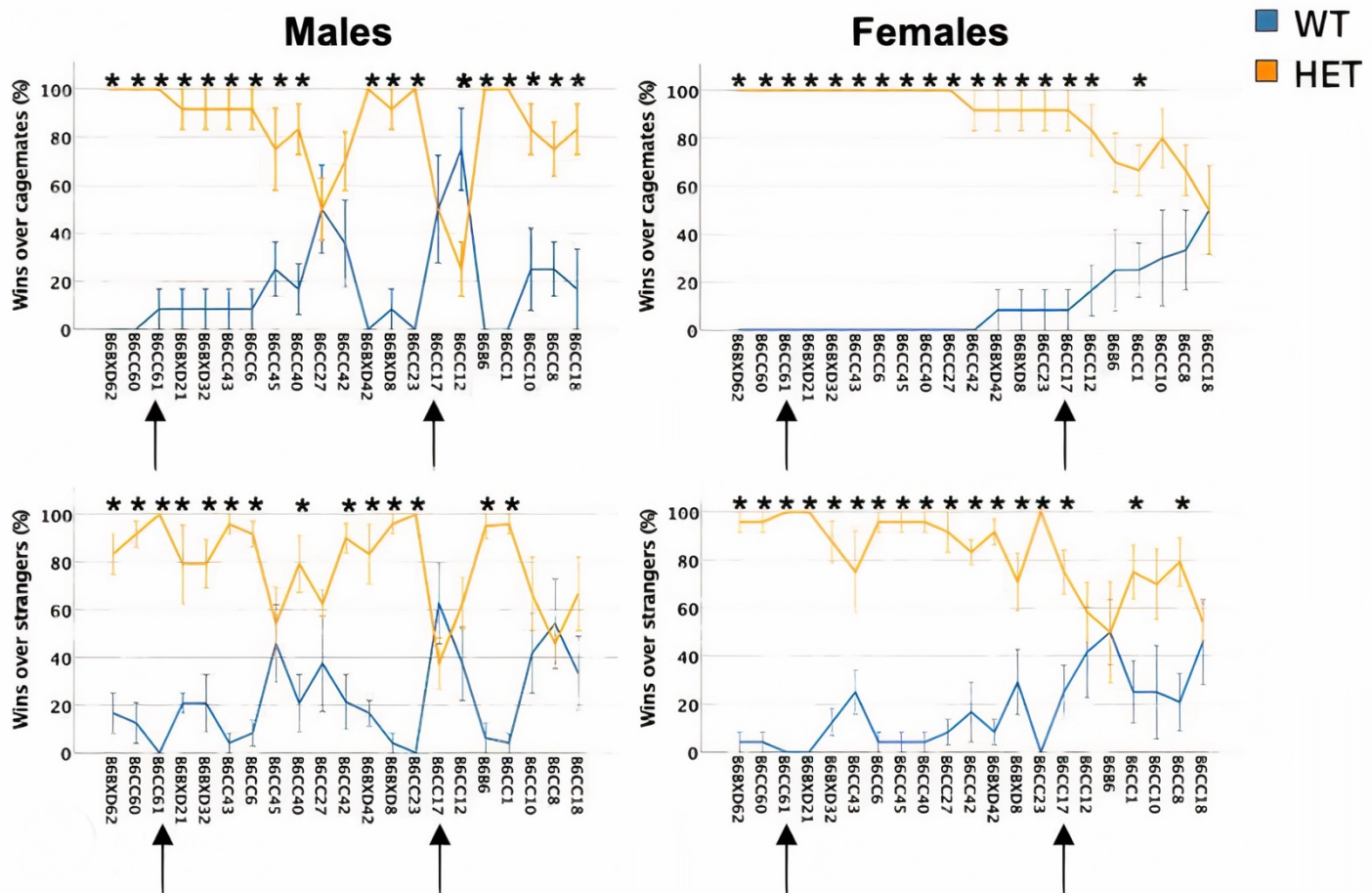


Figure 1. Identifying strains and sexes with differential susceptibility to social dominance due to Chd8 haploinsufficiency. The percentage of social dominance wins for Chd8^{+/-} (orange lines) and WT (blue lines) males (left graphs) and females (right graphs) across 33 GRP stains and separated by trials between cagemates (top graphs) and between strangers in different cages (bottom graphs). The black arrows highlight B6-CC61 and B6-CC17 males and females. Note that social dominance in B6-CC17 males was not significantly different between Chd8^{+/-} and WT cagemates and strangers. Mean +/- standard error of the mean (SEM) is graphed for each group. * $p<.05$ from ANOVA. Figure adapted with permission from [9].

heterozygosity, genetically diverse recombinant inbred strains were leveraged, mainly from the Collaborative Cross (CC) GRP, in a prior study [9] to model the breadth of variety in human genomes. Researchers found that genetic background regulated differential susceptibility to trait disruptions to *Chd8* haploinsufficiency [9]. In this study, two strains that were identified to have differential susceptibility to social dominance due to *Chd8* mutations were investigated for cerebellum volume differences. Literature has shown that the cerebellum, long been noted to control motor behavior, regulates social behavior through its interactions with other brain regions [1]. The effect of *Chd8* haploinsufficiency on the cerebellar volumes of males and females in the B6-CC17 and B6-CC61 mouse strains were leveraged to investigate a relationship between function and structure. Previously, we showed that B6-CC61 males were susceptible to increased social dominance due to *Chd8* haploinsufficiency while males from the B6-CC17 strain were not impacted [9]; **Figure 1**). Females from both strains were susceptible to increased social dominance due to *Chd8* haploinsufficiency and were also included in this study to investigate sex differences [9]. We hypothesized that there was a relationship between strains and sexes with extreme social dominance behavior and their cerebellar brain structure which would be differentially impacted alluding to a structure-function relationship between the cerebellum and social dominance susceptibility due to *Chd8* haploinsufficiency.

Material and Methods:

A. Subjects

All mice in this study were housed in standard cages within the University of Southern California's (USC) University Park Campus (UPC) at the Ray R. Irani vivarium.

Dams were C57BL/6J (B6) mice heterozygous for *Chd8* (*Chd8+/-*). The B6-*Chd8* genotype was created through Cas9 germline editing and previously validated [10]. The *Chd8+/-* mice descended from a founder with loss of function *Chd8* allele with an exon-1 deletion of 7 nucleotides. CC61 and CC17 males from the Collaborative cross (CC) GRP were chosen as sires based on a previous study that revealed differential susceptibility to social dominance in the F1 male offspring [9]. Due to this breeding strategy, the *Chd8* protein expression was reduced by 50% in *Chd8+/-* subjects compared to WT littermates. Both males and females were included in this study. Two cohorts of subjects were included in this study; about half of the subjects were assigned to Cohort 1 and tested in the social dominance tube test prior to in vivo MRI scanning. The remaining subjects in Cohort 2 were also scanned in the MRI but not tested for social dominance. Researchers were blinded to the *Chd8* genotype throughout all stages, including behavioral testing, MRI scanning, and brain volume quantification. Additional precautionary measures included randomization of the mice strains testing order and separation of the sexes to avoid confounding variables. These studies were conducted between the typical light cycle of 6 am PST and 5 pm PST with 45 minutes to acclimate to the behavioral room before the onset of each behavioral test. Housing conditions consisted of 4 mice per each cage including 2 WT and 2 *Chd8+/-* mice of the same strain and sex in each cage.

B. Behavioral Experiment (Social Dominance Tube Test)

The social dominance test (**Figure 2**). measures socially dominant mice over a same-sex and strain conspecific of the opposite *Chd8* genotype. This was done by placing *Chd8+/-* and WT mice that were similar in age and weight (n=5-7 subjects per strain and sex group) into opposing openings of a narrow clear, plastic tube received from ePlastics. The specific tube size was chosen based on the

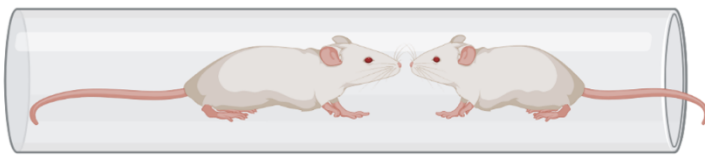


Figure 2. Social dominance tube test.

size of the strain to ensure unidirectional movement. The sizes in inches were either 1.250 (outer diameter) by 1.000 (inner diameter), 1.250 (outer diameter) by 1.125 (inner diameter), or 1.500 (outer diameter) by 1.250 (inner diameter). For each subject, two researchers coordinated to orient the subject's nose to the center of the tube, allowing them to meet towards the middle of the tube. Since the tube was too narrow for the subject to turn around or pass by the opposing subject, a mouse would have to back out of the tube or be pushed out of the tube first and hence be labeled as a "loss" while its counterpart remaining in the tube would've been labeled as a "win." Two days prior to testing, each mouse ran through the tube by itself for 10 practice runs for habituation purposes. In these cases, a flat rubber rod was used to prevent them from backing out and to reinforce running forward through the tube. After habituation, every mouse underwent 6 social dominance trials with a mouse of the opposite Chd8 genotype: 4 trials against strangers from separate cages followed by 2 trials between their cage mates.

C. Cerebellum Quantification

The Small Animal Imaging Core affiliated with the Children's Hospital of Los Angeles (CHLA) performed MRI scans on B6-CC61 and B6-CC17 males and females which included a total of 99 mice. Cohort 1 included a total of 46 subjects and Cohort 2 included 55 subjects. All mice were transferred from UPC to CHLA for MRI scanning after habituating at CHLA for at least a month. The mice were anesthetized using isoflurane through a nose cone and held in place using ear bars. All experiments in the study were done in accordance with ethical guidelines for animal

studies and following protocols approved by the Institutional Animal Care and Use Committee at USC and CHLA. After stabilizing the mouse in a chest-down position to ensure the correct orientation of the brain, a software called PARAVISION was employed to obtain the scanned MRI images. Subjects from Cohort 1 and 2 were treated identically except that Cohort 1 underwent standard resolution and a higher resolution was used for Cohort 2. Finally, to quantify the MRI scans, AMIRA 3D software was used to manually outline the scans and obtain area per slice. The Allen Brain Atlas was used as a reference for the segmentation of cerebellum and total brain volume. The brain scans were first uploaded as a DCM file onto AMIRA, and the lasso tool was used to outline the cerebellum for Cohorts 1 and 2. The total brain volume was also quantified for Cohort 2 by using the lasso tool and outlining the entire brain slice. The generated data was then copied into an excel sheet. For Cohort 1, the measured area per slice was multiplied by 0.375 to calculate volume (mm^3) due to the fact the slices are 355 microns thick with a 20-micron gap between each slice. For Cohort 2, the measured area per slice was multiplied by .224 to calculate volume given the higher resolution MRI used thinner mice coronal brain slices. To ensure consistent definitions for the cerebellum, 7 mice of the first cohort were segmented again to ensure that both volumes were within 5% of each other before beginning the second cohort.

D. Statistical Analysis

Chi-squared tests were employed to determine differences in social dominance between Chd8 genotype groups within each strain and sex group in Cohort 1. A three-way analysis of variance (ANOVA) with Chd8 genotype, strain, and sex as fixed factors was employed to test for significant main effects of Chd8 genotype on cerebellar volumes for subjects in Cohorts 1 and 2 and total brain volumes in Cohort 2 subjects. A Shapiro-wilk test was conducted to support the use of

parametric tests given data normality for the cerebellum and total brain volumes. The parametric test results reported include F and p-values from ANOVA and Cohen's D included as strength of effect measures. The statistical analyses and computations were completed in SPSS and Excel. To create the figures and graphs, BioRender and SPSS were used. Effect size estimates: The central effect size included in the tables is Cohen's D. This was calculated individually for both B6-CC61 and B6-CC17 males and females by subtracting the mean recorded value for Chd8+/- mice from the mean recorded value for the Chd8 WT mice within a strain and sex. To calculate Cohen's D, the mean differences were divided by the pooled standard deviation.

Results:

A. Differential susceptibility to social dominance due to Chd8 haploinsufficiency based on strain and sex

Between-Subjects Factors				
Sex	Strain		N	
F	B6-CC17	Strain	B6-CC17	10
		Genotype	HET	5
			WT	5
	B6-CC61	Sex	F	10
		Strain	B6-CC61	10
		Genotype	HET	4
M	B6-CC17		WT	6
		Sex	F	10
		Strain	B6-CC17	10
	B6-CC61	Genotype	HET	5
			WT	5
		Sex	M	10
	B6-CC17	Strain	B6-CC61	10
		Genotype	HET	8
			WT	8
	B6-CC61	Sex	M	16
		Strain	B6-CC61	10
		Genotype	HET	8
			WT	8
		Sex	M	16

Table 1. Cohort 1 subject numbers by strain, sex, and Chd8 genotype. The analysis carried out in the entire experiment is dependent on knowing the number of mice in each of these categories. F = female; M = male; WT = wild-type; HET = Chd8+/-; N = number of subjects.

Between-Subjects Factors				
Sex	Strain		N	
F	B6-CC17	Strain	B6-CC17	15
		Genotype	HET	7
			WT	8
	B6-CC61	Sex	F	15
		Strain	B6-CC61	13
		Genotype	HET	5
M	B6-CC17		WT	8
		Sex	F	13
		Strain	B6-CC17	15
	B6-CC61	Genotype	HET	8
			WT	7
		Sex	M	15
	B6-CC17	Strain	B6-CC61	12
		Genotype	HET	6
			WT	6
	B6-CC61	Sex	M	12
		Strain	B6-CC61	12
		Genotype	HET	6
			WT	6
		Sex	M	12

Table 2. Cohort 2 subject numbers by strain, sex, and Chd8 genotype. The analysis carried out in the entire experiment is dependent on knowing the number of mice in each of these categories. F = female; M = male; WT = wild-type; HET = Chd8+/-; N = number of subjects

The social dominance tube tests between cagemates and strangers were analyzed for significant differences with chi-squared and magnitude of difference with Cohen's D, separately as well as the combined average percentage of social dominance wins across cagemates and strangers (**Table 3**). B6-CC17 female Chd8+/- mice were socially dominant between strangers ($X^2 (3, 10) = 7.33, p = 0.0048$) and cagemates ($X^2 (2, 10) = 8.00 p = 0.016$) compared to their WT counterparts. Additionally, B6-CC61 female Chd8+/- mice were also socially dominant between strangers ($X^2 (3, 10) = 10.0, p = 0.010$) and cagemates ($X^2 (1, 10) = 10.0 p = 0.005$) compared to their WT counterparts. B6-CC61 Chd8+/- male mice also showed social dominance over WT strangers ($X^2 (4, 16) = 9.33, p = 0.041$) and cagemates ($X^2 (2, 16) = 10.0, p = 0.004$). The combined social dominance averaged over cagemates and strangers revealed greater social dominance in Chd8+/- mice over WT counterparts in B6-CC17 females ($X^2 (3, 10) = 10.0, p = 0.016$), B6-CC61 females ($X^2 (3, 10) = 10.0, p = 0.010$),

		Males						
		WT N	WT Mean	WT St. Dev	Het N	Het Mean	Het St. Dev	Cohen's D
Average percentage of social dominance wins	B6-CC17	5	40.000	0.374	5	60.000	0.141	0.791
	B6-CC61	6	17.000	0.105	6	83.000	0.333	2.928
Social Dominance Cagemates	B6-CC17	5	0.400	0.548	5	0.600	0.418	0.459
	B6-CC61	6	0.083	0.204	6	0.917	0.204	4.473
Social Dominance Strangers	B6-CC17	5	0.467	0.447	5	0.567	0.279	0.300
	B6-CC61	6	0.208	0.188	6	0.792	0.401	2.042
Females								
		WT N	WT Mean	WT St. Dev	Het N	Het Mean	Het St. Dev	Cohen's D
Average percentage of social dominance wins	B6-CC17	5	16.000	0.089	5	88.000	0.268	4.031
	B6-CC61	6	3.000	0.068	4	96.000	0.083	14.054
Social Dominance Cagemates	B6-CC17	5	0.100	0.224	5	0.900	0.224	4.000
	B6-CC61	6	0.000	0.000	4	1.000	0.000	N/A
Social Dominance Strangers	B6-CC17	5	0.183	0.171	5	0.867	0.298	3.145
	B6-CC61	6	0.042	0.102	4	0.938	0.125	9.005

Table 3. Percentage of social dominance wins averaged between cagemates and strangers, between only cagemates, and between only strangers plotted by strain and sex. The social dominance scores were measured in the social dominance tube test for males (top table) and females (bottom table).

and B6-CC61 males ($X^2 (4, 16) = 8.8, p = 0.048$). However, there were no significant differences between B6-CC17 *Chd8+/-* males compared to B6-CC17 WT males (**Table 3**). Females showed a greater difference, as revealed by Cohen's D effect sizes, between *Chd8+/-* and WT for both strains compared to the males which showed a lack of statistical significance in B6-CC17 (**Table 3**).

B. *Chd8* heterozygous mice show enlarged cerebellar volumes

Cohort 1:

The number of subjects in each group for standard-resolution MRI in Cohort 1 are listed in Table 1. Cohort 1 showed no significant difference in cerebellum volume

between WT and *Chd8+/-* mice for B6-CC17 females ($F_{1,13} = 0.068, p = 0.800$) and B6-CC17 males ($F_{1,8} = 0.184, p = 0.679$). There were significantly increased cerebellum volumes in *Chd8+/-* mice compared to WT for B6-CC61 females ($F_{1,8} = 22.0, p = 0.002$) with a large effect size ($d = 3.39$; **Table 4**). There were no significant differences between *Chd8+/-* and WT cerebellar volumes for B6-CC17 females, B6-CC17 males, and B6-CC61 males. B6-CC61 females had a larger effect size than B6-CC61 males ($d = 3.39$ versus 0.99). Cerebellum volumes of *Chd8+/-* models against their WT counterparts for both strains combined were larger in females ($F_{0,19} = 5.9, p = 0.027$) than in males ($F_{0,19} = 5.9, p = 0.027$).

		Males						
		WT N	WT Mean	WT St. Dev	Het N	Het Mean	Het St. Dev	Cohen's D
Cerebellum Volume	B6-CC17	5	61.6	3.88	5	62.66	3.88	0.304
	B6-CC61	8	64.0	3.71	8	67.5	3.54	0.990
		Females						
		WT N	WT Mean	WT St. Dev	Het N	Het Mean	Het St. Dev	Cohen's D
Cerebellum Volume	B6-CC17	5	66.1	4.44	5	66.8	4.45	0.1850551
	B6-CC61	6	65.1	2.81	4	72.2	1.13	3.3871867

Table 4. Cerebellar volume plotted by strain for the standard resolution MRI Cohort 1. The cerebellar volume was measured from the MRI scans of 46 mice and then group averages of cerebellum volume (mm^3) were plotted by strain for WT and *Chd8+/-* males (top table) and females (bottom table).

		Male							
		WT N	WT Mean	WT St. Dev	Het N	Het Mean	Het St. Dev	Cohen's D	
Cerebellum Volume	B6 CC17	7	62.3	2.32	8	65.5	1.95	1.62	
	B6CC61	6	64.8	2.88	6	67.6	2.34	1.17	
		Female							
		WT N	WT Mean	WT St. Dev	Het N	Het Mean	Het St. Dev	Cohen's D	
Cerebellum Volume	B6 CC17	8	66.2	3.18	7	70.7	1.43	1.92	
	B6CC61	8	64.8	2.88	5	71.2	1.80	2.77	

Table 5. Cerebellar volume plotted by strain for the high-resolution MRI Cohort 2. The cerebellar volume was measured from the MRI scans of 46 mice and the group averages of cerebellum volume (mm^3) are shown for WT and Chd8 males (top table) and females (bottom table).

Cohort 2:

The number of subjects in each group for the high-resolution MRI data for Cohort 2 are listed in Table 2. The cerebellar volumes were larger in *Chd8+/-* mice compared to WT including in B6-CC17 males ($F_{1,13} = 8.48, p = 0.012$), B6-CC17 females ($F_{1,13} = 11.8, p = 0.004$), and B6-CC61 females ($F_{1,12} = 17.53, p = 0.002$) with large effect sizes (Table 5). There were no significant differences between cerebellar volumes in B6-CC61 males with different *Chd8* genotypes. Females had larger effect size differences in enlarged cerebellum volumes due to *Chd8* haploinsufficiency

compared to males, particularly in the B6-CC61 strain ($d = 1.17$ versus 2.77). Similar to Cohort 1 results, cerebellum volumes of *Chd8+/-* mice against their WT counterparts for both strains combined were larger in females ($F_{0,27} = 27.40, p < 0.001$) than in males ($F_{0,26} = 10.80, p = 0.003$).

C. Enlarged brain volumes in *Chd8+/-* males and females in the B6-CC61 strain but not B6-CC17

Total brain volumes from Cohort 2 subjects showed significant enlargement of the brain in B6-CC61 *Chd8+/-* females

		Male							
		WT N	WT Mean	WT St. Dev	Het N	Het Mean	Het St. Dev	Cohen's D	
Total Brain Volume	B6 CC17	7	506	5.91	8	513	36.8	0.284	
	B6CC61	6	536	22.9	6	555	12.3	1.14	
		Female							
		WT N	WT Mean	WT St. Dev	Het N	Het Mean	Het St. Dev	Cohen's D	
Total Brain Volume	B6 CC17	8	507	58.3	7	524	41.0	0.350	
	B6CC61	8	548	13.9	5	572	19.1	1.65	

Table 6. Total brain volume plotted by strain for the high-resolution MRI Cohort 2. The brain volume was measured from the MRI scans of 46 mice and the group averages of brain volume (mm^3) are shown for WT and *Chd8+/-* males (top table) and females (bottom table).

($F_{1,12} = 7.32, p < 0.05$) and males ($F_{1,11} = 2.857, p < 0.122$) compared to WT (**Table 6**). In contrast, total brain volume for B6-CC17 *Chd8+/-* males and females were not significantly different than WT controls (**Table 6**).

Discussion:

In this study, we investigated the relationship between cerebellar volume, social dominance and the *Chd8* genotype of mice. We found the presence of a *Chd8* genotype effect as *Chd8+/-* mice from some strain and sex groups show enlarged cerebellar and total brain volumes, consistent with *CHD8*'s implication in macrocephaly. In Cohort 1 (standard resolution MRI), the B6-CC61 strain showed cerebellum enlargement in females while the B6-CC17 strain remained resilient in both sexes. This was not consistent with Cohort 2 (high-resolution MRI) which showed significant enlargement of the cerebellum in both sexes of the B6-CC17 and B6-CC61 females. Differences in results between cerebellum volumes in mice from Cohort 1 and Cohort 2 may be attributed to both an increase in imaging quality in Cohort 2 compared to Cohort 1 as well as differences in the age of the mice. However, B6-CC17 in Cohort 2 shows cerebellum enlargement despite this strain showing resilience to social dominance. On the other hand, the B6-CC61 strain showed significant enlargement of cerebellum in both cohorts, which corresponds with the social dominance tube experiment in which this strain was 100% dominant over their WT counterparts. With regard to total brain volume, there was significant enlargement for both sexes of the B6-CC61 strain while the B6-CC17 showed insignificant changes.

In addition to the genotypic and strain differences, sex also played a major role. Female *Chd8+/-* mice had the largest cerebellar volume and showed a 5.3% and 7.6% enlargement over their male counterpart in the B6-CC61 and B6-CC17 strains respectively. Although these numbers

seem relatively minute, in the context of NDD, a hippocampal volume reduction of 2-4% is associated with psychosis in schizophrenia, a testament to the sensitivity and complexity of the brain [11].

Using diverse genetic models in research will enhance the probability of successful translation in a clinical population, a challenge NDD research currently faces. Furthermore, it provides researchers with the opportunity to understand the individual differences in symptom etiologies as well as the genetic and molecular pathways underlying susceptibility and resilience. The CC GRP employed in this research is a powerful tool as it captures approximately 90% of the genetic variation in the 3 major subspecies of house mice (*Mus musculus*) covering over 40 million single nucleotide polymorphisms (SNPs) [12]. Given the breadth of human genetic diversity, thorough research must be conducted on the influence of genetic background on behavioral phenotypes in NDDs. This is especially pertinent to a disorder such as autism which is often studied using single inbred strains, primarily B6, despite the disorder being clinically and genetically heterogeneous. Recent research conducted on induced pluripotent stem cells shows significant advances in the development of an accurate model to investigate disease etiopathogenesis which will enhance the likelihood of successfully translating work from mice to human models. In the context of *CHD8*, there is an influence of the iPSC's host's genetic background in regulating the effect of *CHD8* haploinsufficiency on excitatory and inhibitory neuronal growth in cortical neurons [8]. This is then appropriate to relate cortical excitations and inhibitions with specific clinical symptoms and the extent of their severity. This study supports the premise of these studies given that this data shows genetic diversity can serve as a model for uncovering structural differences and identifying resilient and susceptible strains.

To further this study, ongoing analyses are testing the relationship between social dominance and brain volumes more directly by relating the cerebellar volumes of the specific mice that were tested in the social dominance tube test to their performance in the test. Furthermore, the total brain volume for B6-CC17 males and females did not show a significant *Chd8* genotype effect while B6-CC61 did with large effect sizes. This must be corroborated with additional strains that also exhibit similar levels of differential impact in the social dominance tube experiment. The discrepancy between the social dominance experiments and brain region analysis is a testament to the difficulty in neurostructural imaging studies since there are countless other genes and brain regions that play a major role in these phenotypes. Therefore, future research can include additional brain regions with known ties to social dominance such as the medial prefrontal cortex, dorsal medial thalamus, lateral hypothalamus, and the ventral tegmental area to compare the structural changes of a well-documented socially implicated circuit and the relationship to the cerebellum. Additionally, examining the molecular and circuit detail of the cerebellum including neurotransmitter release and projections to various brain regions in *CHD8* versus WT models. This could aid in understanding the potential for volume differences of specific brain regions to represent susceptibility or resiliency to social dominance behaviors which are regulated by many brain regions.

References:

- [1] Carta, I., Chen, C. H., Schott, A. L., Dorizan, S., & Khodakhah, K. (2019). Cerebellar modulation of the reward circuitry and social behavior. *Science*, 363(6424), eaav0581. <https://doi.org/10.1126/science.aav0581>
- [2] Kasari, C., Brady, N., Lord, C., & Tager-Flusberg, H. (2013). Assessing the minimally verbal school-aged child with autism spectrum disorder. *Autism Research*, 6(6), 479–493. <https://doi.org/10.1002/aur.1334>
- [3] Leigh, J. P., & Du, J. (2015). Brief Report: Forecasting the Economic Burden of Autism in 2015 and 2025 in the United States. *Journal of Autism and Developmental Disorders*, 45(12), 4135–4139. <https://doi.org/10.1007/s10803-015-2521-7>
- [4] Bernier, R., Golzio, C., Xiong, B., Stessman, Holly A., Coe, Bradley P., Penn, O., Witherspoon, K., Gerdts, J., Baker, C., Vulto-van Silfhout, Anneke T., Schuurs-Hoeijmakers, Janneke H., Fichera, M., Bosco, P., Buono, S., Alberti, A., Failla, P., Peeters, H., Steyaert, J., Vissers, Lisenka E. L. M., & Francescato, L. (2014). Disruptive CHD8 Mutations Define a Subtype of Autism Early in Development. *Cell*, 158(2), 263–276. <https://doi.org/10.1016/j.cell.2014.06.017>
- [5] Kawamura, A., Katayama, Y., Kakegawa, W., Ino, D., Nishiyama, M., Yuzaki, M., & Nakayama, K. I. (2021). The autism-associated protein CHD8 is required for cerebellar development and motor function. *Cell Reports*, 35(1), 108932. <https://doi.org/10.1016/j.celrep.2021.108932>
- [6] O’Roak, B. J., Vives, L., Girirajan, S., Karakoc, E., Krumm, N., Coe, B. P., Levy, R., Ko, A., Lee, C., Smith, J. D., Turner, E. H., Stanaway, I. B., Vernot, B., Malig, M., Baker, C., Reilly, B., Akey, J.M., Borenstein, E., Rieder, M. J., ... Eichler, E. E. (2012). Sporadic autism exomes reveal a highly interconnected protein network of de novo mutations. *Nature*, 485(7397), 246–250. <https://doi.org/10.1038/nature10989>
- [7] Antaki, D., Guevara, J., Maihofer, A. X., Klein, M., Gujral, M., Grove, J., Carey, C. E., Hong, O., Arranz, M. J., Hervas, A., Corsello, C., Vaux, K. K., Muotri, A. R., Iakoucheva, L. M., Courchesne, E., Pierce, K., Gleeson, J. G., Robinson, E. B., Nievergelt, C. M., & Sebat, J. (2022). A phenotypic spectrum of autism is attributable to the combined effects of rare variants, polygenic risk and sex. *Nature Genetics*, 54(9), 1284–1292. <https://doi.org/10.1038/s41588-022-01064-5>
- [8] Paulsen, B., Velasco, S., Kedaigle, A. J., Pigni, M., Quadrato, G., Deo, A. J., Adiconis, X., Uzquiano, A., Sartore, R., Yang, S. M., Simmons, S. K., Symvoulidis, P., Kim, K., Tsafou, K., Podury, A., Abbate, C., Tucewicz, A., Smith, S. N., Albanese, A., & Barrett, L. (2022). Autism genes converge on asynchronous development of shared neuron classes. *Nature*, 1–6. <https://doi.org/10.1038/s41586-021-04358-6>
- [9] Tabbaa, M., Knoll, A., & Levitt, P. (2023). Mouse population genetics phenocopies heterogeneity of human *Chd8* haploinsufficiency. *Neuron*, 111(4), 539–556.e5. <https://doi.org/10.1016/j.neuron.2023.01>

[10] Platt, R. J., Zhou, Y., Slaymaker, I. M., Shetty, A. S., Weisbach, N. R., Kim, J.-A., Sharma, J., Desai, M., Sood, S., Kempton, H. R., Crabtree, G. R., Feng, G., & Zhang, F. (2017). Chd8 Mutation Leads to Autistic-like Behaviors and Impaired Striatal Circuits. *Cell Reports*, 19(2), 335–350. <https://doi.org/10.1016/j.celrep.2017.03.052>

[11] Nelson, M. D., Saykin, A. J., Flashman, L. A., & Riordan, H. J. (1997). Hippocampal volume reduction in schizophrenia as assessed by Magnetic Resonance Imaging: A Meta-analytic study. *Schizophrenia Research*, 24(1-2), 153. [https://doi.org/10.1016/s0920-9964\(97\)82438-3](https://doi.org/10.1016/s0920-9964(97)82438-3)

[12] Chesler, E. J. (2013). Out of the bottleneck: The diversity outcross and collaborative cross mouse populations in Behavioral Genetics Research. *Mammalian Genome*, 25(1-2), 3–11. <https://doi.org/10.1007/s00335-013-9492-9>

[13] Buescher, A. V. S., Cidav, Z., Knapp, M., & Mandell, D. S. (2014). Costs of Autism Spectrum Disorders in the United Kingdom and the United States. *JAMA Pediatrics*, 168(8), 721. <https://doi.org/10.1001/jamapediatrics.2014.210>

[14] Yasin, H., & Zahir, F. R. (2020). Chromodomain helicase DNA-binding proteins and neurodevelopmental disorders. *Journal of Translational Genetics and Genomics*, 4(4). <https://doi.org/10.20517/jtgg.2020.30>

Behavioral Assessment of Sex Differences in the Tg-F344-AD Rat Model of Alzheimer's Disease

Charlotte Stiplosek¹, Alicia Quihuis¹, Christian Pike²

¹USC Dana and David Dornsife College of Letters, Arts and Sciences

²USC Leonard Davis School of Gerontology

Abstract:

Alzheimer's disease (AD) is characterized by progressive neuropathology that leads to memory impairments, dementia and eventually death. Studies have shown that women have a higher prevalence of AD. Animal research has revealed a relationship between sex differences in the AD-like pathology and associated behavioral deficits. To further investigate this sex bias, we used the TgF344-AD (Tg) rat model that exhibits an extensive range of AD-related neuropathology: age-dependent amyloidosis, neuroinflammation, neurofibrillary tangles, and neuronal death.

We investigated potential sex differences in the TgF344-AD rat through a series of behavioral assessments at various ages. Specifically, we assessed performance on Novel Object Recognition and Barnes Maze behavioral tasks to observe their short-term and long-term memory, respectively, at ages 5-7 months and 20-22 months. These behavioral assays informed the relationship between sex and progressive memory deficits, in addition to providing more evidence about progressive memory loss of AD.

Introduction:

Alzheimer's disease (AD) is a neurodegenerative disorder of aging that affects 6.7 million Americans aged 65 and older (Alzheimer's Association, 2023). AD has distinctive molecular pathology including the accumulation of neurofibrillary tau tangles, composed of hyperphosphorylated tau, and amyloid- β plaques. (Alzheimer's Association, 2023). Further, it is characterized by progressive cognitive decline. Interestingly, AD is more prevalent in females than males

and is associated with numerous sex differences.

In our study, we investigated sex differences in AD by characterizing an animal model of AD cross-sectionally to uncover behaviorally phenotypic sex differences that may demonstrate the appearance of this degenerative disorder. We used the TgF344-AD rat model developed on a Fisher 344 background [1]. This model contains two mutations implicated in AD: overexpression of human amyloid precursor protein (APPsw) and presenilin1 (PSE1E9). These mutations capture human pathological changes due to AD including neurofibrillary tau tangles, amyloid- β plaques, neuronal loss, and gliosis. Further, the TgF344-AD model demonstrates age-dependent cognitive impairment and decline [2][3].

Previous models of AD have demonstrated behavioral sex differences. For example, in the 3xTg-AD model, female mice perform worse than male mice while completing behavioral spatial learning and memory tasks [4]. Sex differences in the TgF344-AD model have not previously been demonstrated, a critical piece of understanding the disparity in human female diagnosis over male diagnosis. This exploration of the TgF344-AD model will demonstrate both genotypic and sex discrepancies in short-term recognition, learning, and spatial memory.

In order to investigate sex differences in short-term working memory, we conducted the Novel Object Recognition Test (NOR), a fast and efficient means of testing phases of learning and memory in rats. We also conducted the Barnes Maze test, a well-established rodent behavioral test to assess

spatial learning and long-term memory [5]. These tasks can provide important insights into variance between sexes of cognitive decline associated with AD-like pathology in the TgF344-AD model.

This behavioral study performs a critical analysis of discrepancies between female and male short-term memory, via Novel Object Recognition Test, and long-term memory, via Barnes Maze Test. Both human data and rodent models elucidate AD is a progressive neurodegenerative disease. Human data has demonstrated a larger diagnosis of females than males, and previous rodent models show that female memory endures larger impact than male memory. We hypothesize TgF344-AD rats will demonstrate short-term and long-term learning and memory deficits, older age groups of TgF344-AD rats will demonstrate cognitive impairment, and females will generally perform worse than males in both short-term memory performance and long-term memory performance.

Materials and Methods:

A. Animals

TgF344-AD rats were generated on a Fischer 344 background by co-injecting rat pronuclei with the following two human genes driven by the mouse prion promoter: “Swedish” mutant human APP (APPsw) and exon 9 mutant human presenilin-1 (PSI E9) [1]. TgF344-AD rats and wild-type (WT) rats were housed under standard conditions with free access to food and water). Subjects were tested cross-sectionally at ages 5-7 months and 20-22 months to display behavior at different phases of cognitive impairment. Novel Object Recognition (NOR) experimental groups include: 5-7m Female WT (n= 6), 5-7m Female Tg (n=9), 5-7m Male WT (n=6), 5-7m Male (n=5), 20-22m Female WT (n=15), 20-22m Female Tg (n=17), 20-22m Male WT (n= 10), and 20-22m Male (n=11). Barnes Maze experimental groups include: 5-7m Female WT (n= 5), 5-7m Female Tg (n=5), 5-7m Male WT (n=4), 5-7m Male (n=7), 20-

22m Female WT (n=9), 20-22m Female Tg (n=9), 20-22m Male WT (n=6), and 20-22m Male (n=9). All animal experiments were performed under an experimental protocol approved by the University of Southern California Institutional Animal Care and Use Committee and performed in strict accordance with National Institutes of Health guidelines and recommendations from the Association for Assessment and Accreditation of Laboratory Animal Care International.

B. Novel Object Behavioral Assay

We assessed the short-term memory of TgF344-AD subjects through the novel object recognition test. The Novel Object Recognition Test (NOR) is a fast and efficient means of testing phases of learning and memory in rats. The test requires three phases: the habituation phase, the learning phase, and the test phase. The habituation phase enables the rat to become familiar with the testing stage. The learning phase involves the visual exploration of two identical objects. The test phase involves replacing one of the previously explored objects with a novel object. Because rodents have an innate preference for novelty, a rodent that remembers a familiar object will spend more time exploring the novel object [6][7][8].

During the habituation phase, the rat is removed from its home cage and placed in the middle of the clear, plastic arena. The dimensions of the arena (width x length x height): 45x45x45 cm open-topped box. The rat then freely explores the arena for 3 minutes. At the end of 3 minutes, the rat is removed and placed in its holding cage. The stage is then cleaned after each subject with 70% vol/vol ethanol. During the learning phase, two identical objects are placed in opposite quadrants of the arena (i.e. NW corner and NE corner). 24 hours after the habituation phase, the rat is placed in the arena, equidistant from both objects. The rat then engages in free exploration for 3 minutes. The testing phase occurs 20 minutes after the learning phase, as a test for short-

term memory. The testing phase employs one object from during the learning phase and one new object of equal height and width; objects are placed in the same locations as learning phase objects, and the rat engages in free exploration for 3 minutes. Exploration activity of the object is quantified as sniffing, mounting, or interaction behavior with the object. No animals were omitted from data analysis.

C. Barnes Maze Behavioral Assay

We assessed hippocampal-dependent spatial reference memory using the Barnes Maze protocol. The Barnes maze is a dry-land-based rodent behavioral test to assess spatial learning and memory [5]. A circular maze with 18 holes was used, and rats were trained to locate a single escape hole. Salient visual cues were positioned on the walls surrounding the maze to encourage spatial awareness. Rats were given three 3-minute trials per day to find their designated escape box that remained in the same location throughout. The first four days were considered the learning phase of the task. The probe acquisition trial was conducted 48 hours after the last training phase on day 7 in which three 3-minute trials were conducted for each rat. The cognitive flexibility trial was conducted on days 8 and 9, in which each animal's escape hole location was rotated 180 degrees from its original location to test their cognitive flexibility. Three 3-minute trials were conducted on days 8 and 9 respectively. The following metrics were measured using EthoVision XT Software (Noldus Information Technology, Wageningen, The Netherlands): time to reach the escape hole (s), number of errors, the velocity of travel (cm/s), and distance traveled (s). No animals were omitted from data analysis.

D. Statistical Quantification and Analysis

Statistical analyses and visualizations were performed using GraphPad Prism. Data are expressed as means \pm standard errors of the mean. The results of behavioral testing

were analyzed by means of non-repeated measures ANOVA and T-test, with a significance value of $p < 0.05$. Males and females were analyzed separately to determine sex difference discrepancies.

Results:

A. Novel Object Recognition

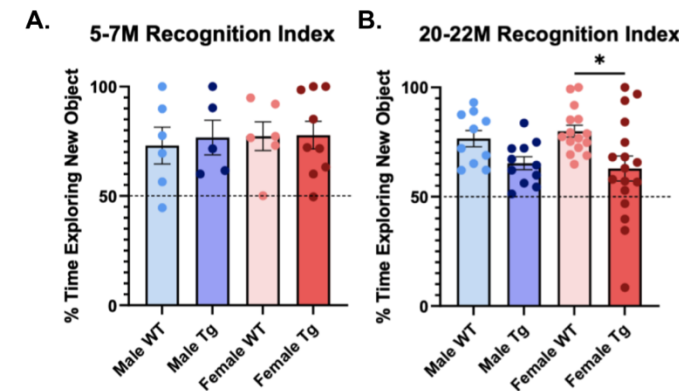


Figure 1. Recognition index measurements for percent time exploring new objects in the NOR task. (A) At 5-7 months, all animals demonstrated similar recognition index. **(B)** At 20-22 months, male WT trended towards a higher recognition index than male Tg. Female WT had statistically significantly larger recognition index than female Tg.

We used the Novel Object Recognition (NOR) behavioral assay to assess cognition and short-term recognition in TgF344-AD rats ages 5-7 and 20-22 months. At 5-7 months, male WT, male Tg, female WT, and female Tg demonstrated a similar recognition index in excess of 50% with a standard deviation of approximately 10% above and below the mean. (**Figure 1a**) At 20-22 months, male WT trended toward a higher recognition index than male Tg. Female WT groups demonstrated a significantly higher recognition index than female Tg groups. (**Figure 1b**).

B. Barnes Maze

The Barnes Maze behavioral assay enabled investigation of long-term memory and spatial memory. To analyze the Barnes Maze behavioral data, we performed an Area Under the Curve (AUC) analysis of the learning period. At 5-7 months, no significant sex or genotypic difference appeared between

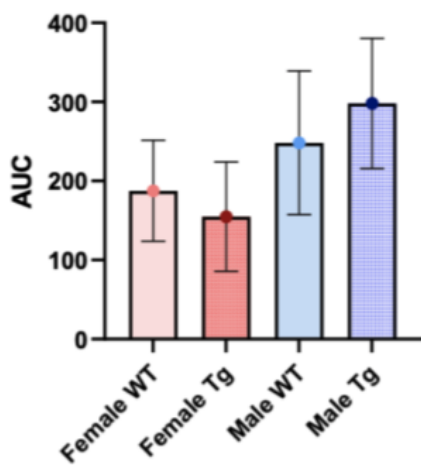
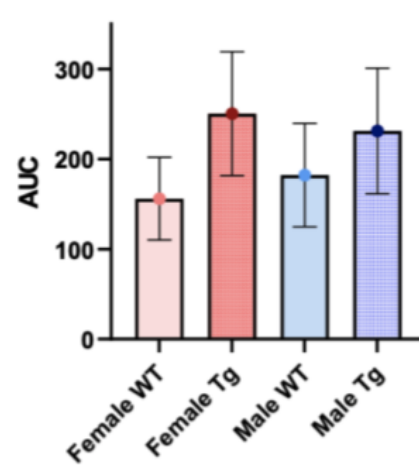
A.**AUC Total Time for Learning Period: 5-7M****B.****AUC Total Time for Learning Period: 20-22M**

Figure 2. AUC measurements for amount of time each group took to complete Barnes Maze learning period tasks. (A) At 5-7 months, male WT and male TG subjects took longer to complete the learning task than female WT and female TG subjects. **(B)** At 20-22 months, female TG and male TG tended to take longer than female WT and male WT, respectively.

groups. Males tended towards larger AUC measurements than females, with male Tg recording the largest AUC measurement. (**Figure 2a**) At 20-22 months, Female Tg trends towards larger AUC readings than female WT. Male Tg AUC readings during the

learning period at 20-22 months also demonstrate larger AUC measurements than male WT groups. (**Figure 2b**).

Probe measurements represent the number of errors and the amount of time, latency, each group requires to complete the

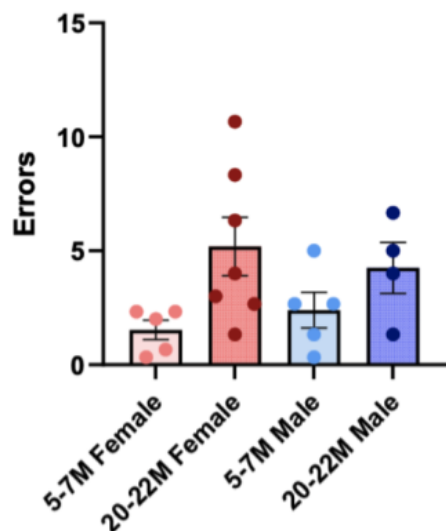
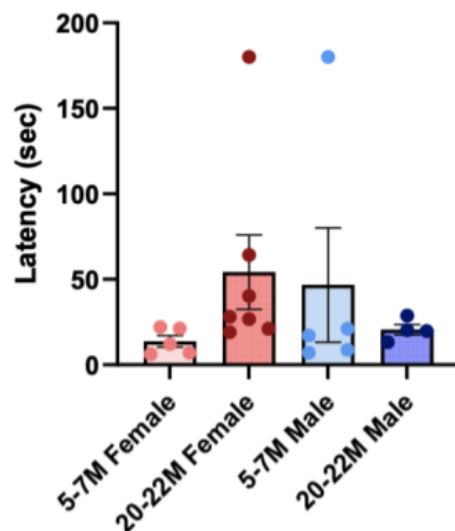
A.**5-7M, 20-22M Tg Errors Probe Day****B.****5-7M, 20-22M Tg Time Probe Day**

Figure 3. Errors and time for Tg subjects to complete Probe Day Barnes Maze long-term memory task. (A) 20-22 month females and males tended to make more errors than 5-7 month females and males, respectively. **(B)** 20-22 month females took longer than 5-7 month females to complete probe day task. 5-7 month males took longer than 20-22 month males to complete probe day task.

task.

At 5-

7

months, female Tg groups trend towards fewer errors and take less time than female Tg groups at 20-22 months. (**Figures 3a, 3b**) Male Tg also demonstrate fewer errors at 5-7 months than at 20-22 months. At 5-7 months, males take more time to complete the task than at 20-22 months. (**Figures 3a, 3b**) All WT animals completed the probe day task, although no significance was displayed.

Discussion:

A. Novel Object Recognition

We used the Novel Object Recognition (NOR) behavioral assay to assess cognition and short-term recognition in TgF344-AD Rats ages 5-7 months and 20-22 months. We assessed subjects' behavior based on the NOR Recognition Index, or the percentage of time each subject spent exploring the novel over the familiar object during the testing phase. The dotted line at 0.50 indicates the chance performance value; the recognition index greater than 0.50 indicates a novelty preference, and thus recognition memory of the previous object in conjunction with a preference for the novel object.

At 5-7 months and 20-22 months, all subjects demonstrated a preference for the novel object as evidenced by all groups performing above the 50% threshold.

At 5-7 months, all subjects performed 25-30% above the 50% threshold which demonstrates that preference for the novel object was not due to chance. The 5-7 month Novel Object Recognition test served as an internal control to assess sex differences prior to the aggregation of transgenic AD pathology. As expected, due to the absence of AD pathology, WT and Tg groups demonstrated similar NOR results. Our results indicate there is no trend or significant sex difference in short-term recognition.

At 20-22 months, full AD-like pathology is present in the TgF344-AD model. All groups performed above the 50% threshold. Male WT explored the novel object more than male Tg, demonstrating more

preference for the novel object than their same sex transgenic age group. Female WT explored the novel object significantly more than the Female Tg group, demonstrating the Female Tg group is cognitively impaired and experiences object recognition deficits for this short-term memory task.

At 20-22 months, once pathology has appeared, there is a genotypic difference between WT and Tg, with WT demonstrating larger explore time for the novel object than Tg groups. This difference appeared as a trend between Male genotypes and was a statistically significant difference between female genotypes thus suggesting AD pathology in Tg males and females leads to impaired short-term recognition and cognitive flexibility.

B. Barnes Maze

The Barnes Maze behavioral test served as an assessment of spatial learning and long-term memory. We performed this behavioral test at ages 5-7 months and 20-22 months.

To assess sex and genotypic differences during the learning period we created AUC figures to demonstrate the mean total time each group took to complete the task during the four-day learning period. A larger AUC measurement denotes further time to complete the learning task.

At 5-7 months, female WT and female Tg groups trended towards less total time to complete the task than male WT and male Tg groups. (**Figure 2a**) This trend postulates a potential sex difference in learning between females and males at 5-7 months in the Tg F344-AD model [9][10].

At 20-22 months, female WT trended to lower AUC measured than female Tg. (**Figure 2b**) Male WT similarly trended towards lower AUC measurement than male Tg groups. (**Figure 2b**) These results suggest genotypic differences between WT and Tg groups once AD pathology is fully present.

We recorded the number of errors and amount of time Tg subjects at 5-7 months and

20-22 months take to complete the probe day task, measuring long-term memory. (**Figures 3a, 3b**)

5-7 month females trended towards fewer errors than 20-22M females, demonstrating cognitive impairment due to the onset of AD-like pathology. (**Figure 3a**) Similarly, 5-7 month males trended towards fewer errors than 20-22 month males, following the onset of AD pathology. These results support previous literature that demonstrate the progressive cognitive decline in the TgF344-AD model of AD.

20-22 month females also took longer than 5-7 month females to complete the probe day task reinforcing that at 20-22 months, females experience deficits in their spatial learning and long-term memory. (**Figure 3b**)

One limitation to this study is the declination in health and resulting death of TgF344-AD subjects at 20-22 months, leading to a lower number of participants in the Barnes Maze behavioral assay. Acquiring more subjects at 20-22 months may provide statistically significant insight between WT and Tg during the learning period and probe day that reinforces the displayed trends.

Conclusion:

In conclusion, our results show there is an impairment in both short-term recognition and spatial memory in the TgF344-AD model at 20-22 months. These findings suggest that AD pathology increases cognitive impairment with age, while decreasing both learning and memory. This model demonstrates the progressive cognitive decline of AD. Both male Tg and female Tg subjects demonstrate clear short-term and long-term memory deficits as evidenced by performance at the same age by WT subjects. Therefore, the TgF344-AD model continues to provide useful information to further investigate the behavioral effects of AD and sex differences implicated by AD.

References:

- [1] Cohen, R. M., Rezai-Zadeh, K., Weitz, T. M., Rentsendorj, A., Gate, D., Spivak, I., Bholat, Y., Vasilevko, V., Glabe, C. G., Breunig, J. J., Rakic, P., Davtyan, H., Agadjanyan, M. G., Kepe, V., Barrio, J. R., Bannykh, S., Szekely, C. A., Pechnick, R. N., & Town, T. (2013). A transgenic Alzheimer rat with plaques, tau pathology, behavioral impairment, oligomeric $\alpha\beta$, and frank neuronal loss. *The Journal of neuroscience : the official journal of the Society for Neuroscience*, 33(15), 6245–6256. <https://doi.org/10.1523/JNEUROSCI.3672-12.2013>
- [2] Berkowitz, L.E., Harvey, R.E., Drake, E. et al. Progressive impairment of directional and spatially precise trajectories by TgF344-Alzheimer's disease rats in the Morris Water Task. *Sci Rep* 8, 16153 (2018). <https://doi.org/10.1038/s41598-018-34368-w>
- [3] Do Carmo, S., & Cuello, A. C. (2013). Modeling Alzheimer's disease in transgenic rats. *Molecular neurodegeneration*, 8, 37. <https://doi.org/10.1186/1750-1326-8-37>
- [4] Gür, E., Fertan, E., Kosel, F., Wong, A. A., Balci, F., & Brown, R. E. (2019). Sex differences in the timing behavior performance of 3xTg-AD and wild-type mice in the peak interval procedure. *Behavioural brain research*, 360, 235–243. <https://doi.org/10.1016/j.bbr.2018.11.047>
- [5] Barnes C. A. (1979). Memory deficits associated with senescence: a neurophysiological and behavioral study in the rat. *Journal of comparative and physiological psychology*, 93(1), 74–104. <https://doi.org/10.1037/h0077579>
- [6] Ennaceur A. (2010). One-trial object recognition in rats and mice: methodological and theoretical issues. *Behavioural brain research*, 215(2), 244–254. <https://doi.org/10.1016/j.bbr.2009.12.036>
- [7] Berlyne, D.E. (1950). Novelty and curiosity as determinants of exploratory behavior. *Br J Psychol*, 41, 68-80.
- [8] Ennaceur, A., & Delacour, J. (1988). A new one-trial test for neurobiological studies of memory in rats. 1: Behavioral data. *Behavioural brain research*, 31(1), 47–59. [https://doi.org/10.1016/0166-4328\(88\)90157-x](https://doi.org/10.1016/0166-4328(88)90157-x)
- [9] Bernaud, V.E., Bulen, H.L., Peña, V.L. et al. Task-dependent learning and memory deficits in the TgF344-AD rat model of Alzheimer's disease: three key timepoints through middle-age in females. *Sci Rep* 12, 14596 (2022). <https://doi.org/10.1038/s41598-022-18415-1>
- [10] Talboom, J. S., West, S. G., Engler-Chiurazzi, E. B., Enders, C. K., Crain, I., & Bimonte-Nelson, H. A. (2014). Learning to remember: cognitive training-

induced attenuation of age-related memory decline depends on sex and cognitive demand, and can transfer to untrained cognitive domains. *Neurobiology of aging*, 35(12), 2791–2802.
<https://doi.org/10.1016/j.neurobiolaging.2014.06.008>

Administration of Mitochondrial-Derived Proteins Provide both Neuroprotective and Neurorestorative Effects in an Animal Model of Parkinson's Disease

Sahar Nangoli¹, Derek Phillips^{1,2}, Giselle Petzinger², Su-Jeong Kim³, Pinchas Cohen³, Michael Jakowec²

¹USC Dana and David Dornsife College of Letters, Arts and Sciences

²USC Keck School of Medicine Department of Neurology

³USC Leonard Davis School of Gerontology

Abstract:

Parkinson's disease is the fastest growing neurodegenerative disorder in the world, with the majority of cases being idiopathic [1]. Mitochondria play an important role in the pathophysiology of Parkinson's disease because deficiencies of mitochondrial respiratory chain complex 1 activity have been observed in the substantia nigra of PD patients. The mitochondria produce energy to drive cellular functions for essentially all biological processes, including the generation of ATP, calcium homeostasis, and apoptosis. Potential therapeutics to combat the development of neurodegenerative diseases are mitochondrial derived proteins (MDPs), specifically, small humanin-like peptide 2 (SHLP2) and K4R (an isoform of SHLP2), which have been associated with lower risk of PD [2]. However, it remains unknown whether these MDPs offer neurorestorative properties. SHLP2 is the MDP localized to Complex 1 of the electron transport chain and may enhance specific aspects of metabolism [3]. More recently, collaborators have discovered SHLP2 and K4R, which have been found to contribute to increased mitochondrial function [4]. If administration of SHLP2 and K4R is able to increase mitochondrial function, and consequently, synaptic plasticity, then it may be used as a neurorestorative treatment. To explore SHLP2 and K4R's ability to provide neurorestoration in a rodent model of mitochondria dysfunction, neurotoxin MPTP was used to selectively inhibit Complex I of mitochondria in dopaminergic midbrain

neurons. Findings from our studies suggest that pharmacological targeting of mitochondrial function through small-mitochondrial derived peptides may provide neurorestorative benefits in models of dopamine depletion, cell death, and ultimately lead to increased levels of synaptic plasticity.

Introduction:

Mitochondrial-derived peptides (MDPs) are vital to mitochondrial health, which includes gene expression, proton pumping activity, and other pathways. However, levels of MDPs decline with age, leading them to be linked heavily with age related diseases [5]. Considering this, administration of MDPs to potentially combat the negative effects of age-related disease is an important space in research, and one targeted with this study. In previous research, administration of MDPs both *in vitro* and *in vivo* has shown positive results, preventing cognitive decline and reducing the risk of age-related disease. [2].

In this study specifically, we investigate MDP small humanin-like peptide 2 (SHLP2) that is localized to complex 1 of the mitochondria and is shown to improve mitochondrial function by increasing mitochondrial respiration [2].

Specifically in Parkinson's Disease, mitochondrial dysfunction has been increasingly proven to contribute to the etiology of the disease, localized to NADH-quinone oxidoreductase, or Complex 1, of the electron transport chain. When the activity of complex 1 is inhibited or interfered with,

there is dopaminergic cell death, directly associated with Parkinson's Disease [6].

Considering the decline of complex 1 activity in a PD model and the increase of complex 1 activity with SHLP2, this MDP was consequently studied in association with Parkinson's Disease. Since SHLP2 levels have already been proven to decline with age and be associated with lower risk of PD, we wanted to study whether this MDP could protect against Parkinson's Disease, and if it could restore levels of physical activity after the onset of Parkinson's Disease.

Materials and Methods:

In order to test for protection against Parkinson's Disease, MDPs SHLP2 and K4R were administered prior to neurotoxin MPTP as shown in **Figure 1**.

To test for restoration against Parkinson's Disease, MDPs SHLP2 and K4R were administered after neurotoxin MPTP as shown in **Figure 2**.

C57BL/6 male mice 8 to 10 weeks of age were purchased from Jackson Labs (Bar Harbor, Maine). 1-methyl-4-phenyl-1,2,3,6-tetrahydropyridine (MPTP) (Selleck Chemicals Co., Houston, TX) prepared to a

concentration of 5 mg/kg free-base in 0.9% saline on the day of use. C57BL/6 mice were injected with either one, two, or four injections of 20 mg/kg free-base MPTP 2 hours apart. 10 days after the last injection of MPTP mice were killed by cervical dislocation and the brain quickly removed and placed on wet ice. Striatal tissues for HPLC analysis and western immunoblotting were collected fresh en bloc corresponding to anatomical regions from bregma 1.20 to bregma 0.60, with borders dorsal to the anterior commissure, ventral to the corpus callosum, medial to the lateral ventricle, and 2.5 mm lateral from midline, and frozen at -80°C until analysis. All procedures utilizing MPTP lesioning and tissue collection were approved by the USC Institutional Animal Care and Use Committee.

HPLC Analysis

The protocol for the HPLC analysis of dopamine and its metabolites was derived from a previous study as outlined in Petzinger et al. 2007, which was further adapted from Irwin et al. 1992 and Kilpatrick et al. 1986 [7][8][9].

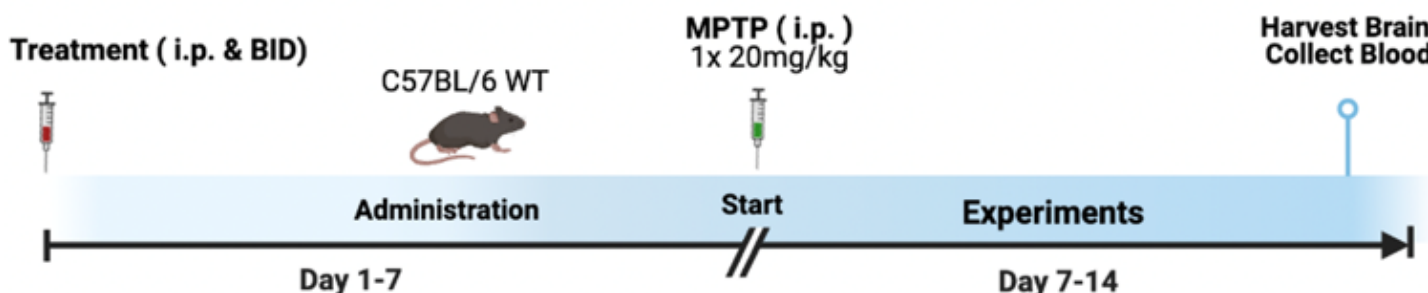


Figure 1. Proposed procedure to test the hypothesis that SHLP2 + K4R provide protection against neurotoxin MPTP.

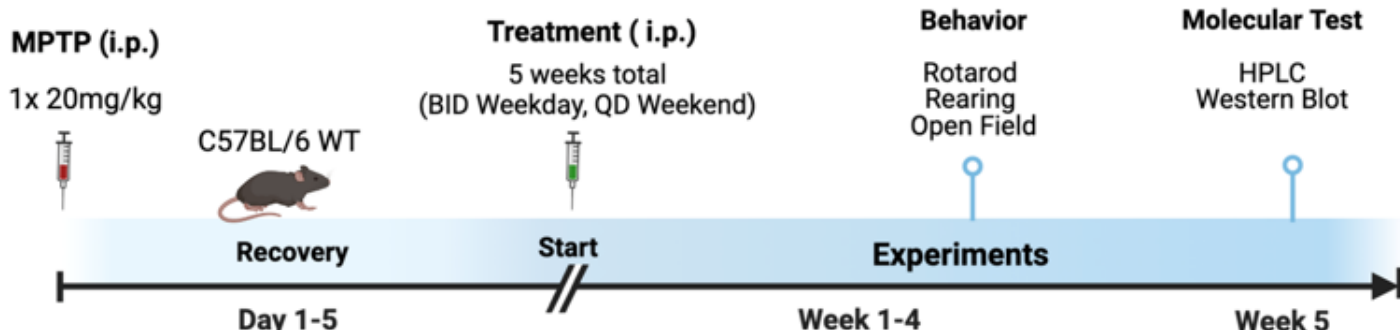


Figure 2. Proposed procedure to test the hypothesis that SHLP2 + K4R provide restoration against neurotoxin MPTP.

Western Immunoblotting

Striatal tissue samples were lysed in RIPA buffer with protease and phosphatase inhibitors (MSSAFE, Sigma), centrifuged at 16,000 x g and the soluble fraction collected for subsequent protein analysis. Total protein content was determined by BCA analysis (ThermoFisher Scientific, XX) and 20 ug of protein resolved on a 10% Tris-Glycine gel by electrophoresis (BioRad, Hercules, CA). Total protein was transferred to nitrocellulose membranes (BioRad), blocked (Genesee Scientific) and probed with the following antibodies overnight at 4°C: Tyrosine hydroxylase (MAB318, Millipore Scientific, XX, XX) and mouse anti-beta actin (1:5000, LI-COR, Cat# 926-42212, RRID: AB_2756372). Membranes were washed, incubated with corresponding goat anti-mouse or goat anti-rabbit conjugated near-infrared secondary fluorescent antibodies (1:5000, LI-COR, Cat# 926-32211, RRID: AB_621843; and Cat# 926-68070, RRID: AB_10956588), and scanned on an Odyssey imaging system (Licor, XX). Relative protein expression was quantified by optical density and normalized to beta-actin as loading control using the Licor imaging program.

Results:

To assess the neuroprotective qualities of SHLP2 and K4R against exposure to neurotoxin MPTP, we treated mice with saline (WT) or K4R SHLP2. We then assessed dopaminergic cell loss via dopamine levels of the striatum using reverse-phase HPLC-electrochemical detection. Results will suggest whether MDPs can prevent the expected reductions in dopamine as a result of MPTP. MPTP (20mg/kg) induces a significant decrease in dopamine levels in the striatum of injected mice (**Figure 3**). As shown, K4R and SHLP2 (2.5mg/kg) protect against MPTP dopamine loss in the striatum in comparison to MPTP (**Figure 3**).

To assess neurorestoration, we investigated whether SHLP2 could rescue dopaminergic neurons after the

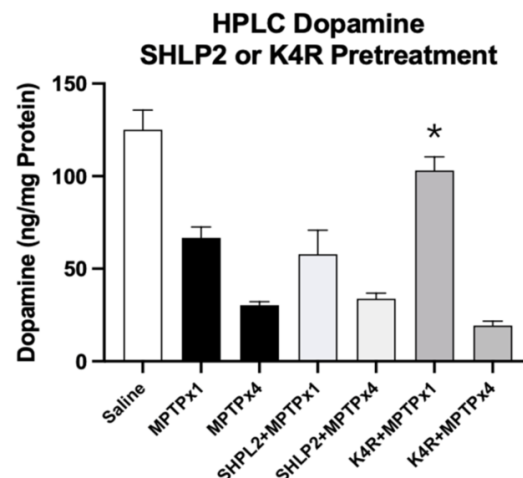


Figure 3. Dopamine levels in the striatum of mice with pretreatment of mitochondrial derived peptides. * refers to the comparison of K4R+MPTPx1 in comparison to MPTPx1.

administration of MPTP. The levels of tyrosine hydroxylase (TH) in the striatum of the mice were examined in western blotting to reveal that K4R and SHLP2 restored TH levels in MPTP-lesioned mice (**Figure 4**). However, SHLP2 on its own did not restore levels of TH in the mice. In both graphs looking at dopamine and tyrosine hydroxylase, administration of SHLP2 and K4R has increased success in neurorestoration and neuroprotection in comparison to SHLP2 on its own.

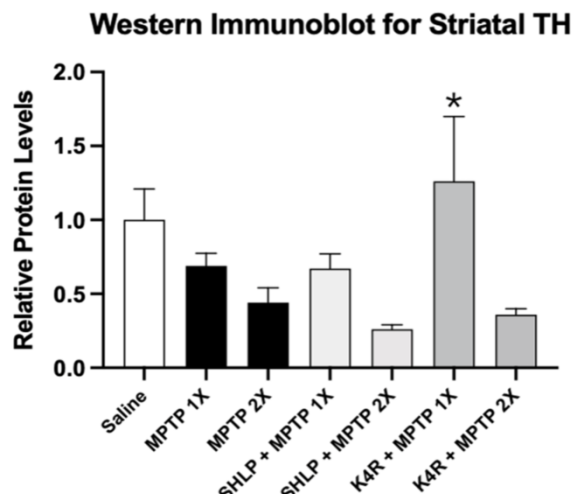


Figure 4. Tyrosine hydroxylase expression in the striatum of mice with post-treatment of mitochondrial derived peptides. * refers to the comparison of K4R+MPTPx1 in comparison to MPTPx1.

Additionally, mice that have had the administration of SHLP2 and K4R after neurotoxin MPTP have significantly increased latency to fall in comparison to those that only have MPTP (**Figure 5**).

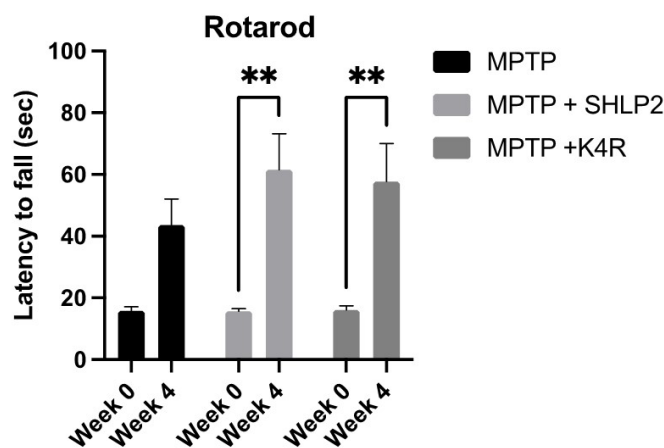


Figure 5. Rotarod learning for mice with post-treatment of mitochondrial derived peptides. ** refers to...

In order to test for the synaptic plasticity in mice that had administration of MDPs after MPTP, we used PSD-95, a postsynaptic marker of plasticity (**Figure 6**). Mice with K4R and SHLP2 have increased levels of PSD-95 compared to WT, the deviation of PSD-95 values within individual groups shows a lack of uniform protein levels. Therefore, this deviation should be taken into account when comparing MDP models to WT.

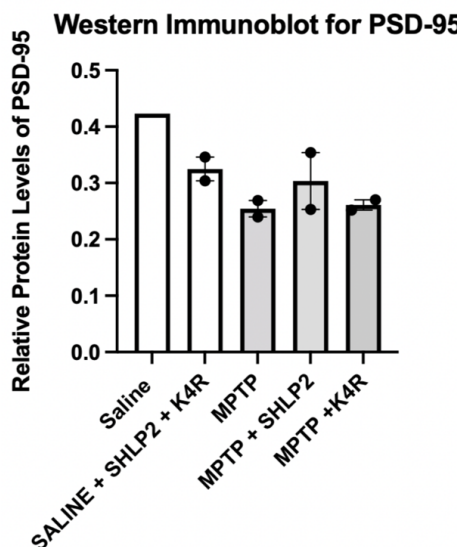


Figure 6. Relative PSD-95 levels in mice models with treatment of MDPs after MPTP.



Figure 7. Western immunoblot Licor imaging demonstrating relative PSD-95 levels in neurorestorative rodent models.

Discussion:

Mitochondrial peptide SHLP2 is localized to complex 1 of the mitochondria, a complex whose activity is significantly inhibited in a PD model. The increased levels of SHLP2 that are associated with lower risk of PD provide supporting evidence that SHLP2 stabilizes complex 1 in a PD model. This study provides evidence that SHLP2 and K4R stabilize the decline of the mitochondria activity during Parkinson's Disease through evidential markers of PD including dopamine levels, TH levels, and motor function. Treatment of SHLP2 and K4R increases mitochondrial membrane potential, especially in comparison to WT mice. This study provides evidence that mitochondria derived peptides are vital to understanding prevention and restoration in relation to Parkinson's Disease.

The stabilizing effects of MDPs, showcased through evidential markers of PD, is outlined in this study. Perhaps most significant is the increased latency to fall observed in **Figure 5** by treatment groups with injections of MDPs. Mice who suffer the negative effects from MPTP can alleviate their motor dysfunction by receiving MDP injections after MPTP. This is consistent

across both SHLP2 and K4R with MPTP in comparison to MPTP only. Although this applies to alleviating mitochondrial dysfunction after the onset of MPTP, we also observed preventing dysfunction in a PD model.

Administering MDPs prior to MPTP can protect against PD onset. Levels of striatal dopamine are used to quantify this – mice with administration of K4R, for example, prior to MPTP, observe striatal dopamine levels significantly higher than the MPTP model. Mice with pretreatment of MDPs prior to MPTP show levels of dopamine that are about 10 mg/kg lower than saline as shown in **Figure 3**.

This is extremely important to the future of studying age-related neurodegenerative disease. This is because mitochondrial derived proteins, which are associated with age, muscle, and mitochondrial health, have a clearly direct relationship with neurodegenerative disease. The decreased levels of MDPs with increased age, and increased risk of PD with increased age tells researchers that increasing MDP expression may decrease PD risk. Not only can the risk of PD be lowered, but after the onset of PD, its negative effects, as suggested by this study, can be alleviated to an extent. Evidence for full function repair is not showcased by the data in this study, however, in future studies, we hope to elongate the duration of observation and increase the dosages of MDPs to see if increased repair is observed.

Mitochondrial derived peptides K4R and SHLP2 are associated with lower risk of PD. In this study, we provide evidence that increased levels of these MDPs provide protective effects in cases of PD and help alleviate and restore motor dysfunction associated with the onset of PD.

Conclusion:

We found that the MDPs SHLP2 and K4R, offer a potential therapeutic to target mitochondria dysfunction in dopaminergic

neurons. SHLP2 and K4R administration increased levels of dopamine uptake and increased levels of tyrosine hydroxylase when administered prior to MPTP. After MPTP administration, SHLP2 and K4R improved rotarod performance and learning rate. These studies highlight the role of K4R and SHLP2 against mitochondrial dysfunction *in vivo* and provide a basis for developing novel therapeutic targets in PD.

In the future, we will run more samples in order to run statistical analyses to help establish the relationship between how MDPs may prevent PD onset and restore function in a PD model. We will also look at other proteins of interest involving synaptic plasticity. Additionally, our lab will explore the synergistic effects of mitochondrial derived proteins and exercise in healthy mice and MPTP mice. Physical exercise benefits are associated with increased energy expenditure and mitochondrial metabolism. We hypothesize that MDPs will increase motor and cognitive performances in PD models.

References:

- [1] Dorsey, E. R., Sherer, T., Okun, M. S., & Bloem, B. R. (2018). The Emerging Evidence of the Parkinson Pandemic. *Journal of Parkinson's disease*, 8(s1), S3–S8. <https://doi.org/10.3233/JPD-181474>
- [2] Kim, S. J., Devgan, A., Mehta, H. H., & Cohen, P. (2019). Mitochondrial-derived peptide, SHLP2, a novel protective factor in Parkinson's disease. *Innovation in Aging*, 3(Suppl 1), S838. <https://doi.org/10.1093/geroni/igz038.3088>
- [3] Kim, S. J., Xiao, J., Wan, J., Cohen, P., & Yen, K. (2017). Mitochondrially derived peptides as novel regulators of metabolism. *The Journal of physiology*, 595(21), 6613–6621. <https://doi.org/10.1113/JP274472>
- [4] Miller, B., Kim, S. J., Kumagai, H., Yen, K., & Cohen, P. (2022). Mitochondria-derived peptides in aging and healthspan. *The Journal of clinical investigation*, 132(9), e158449. <https://doi.org/10.1172/JCI158449>
- [5] Kim, S. J., Miller, B., Kumagai, H., Silverstein, A. R., Flores, M., & Yen, K. (2021). Mitochondrial-derived peptides in aging and age-related diseases.

GeroScience, 43(3), 1113–1121.
<https://doi.org/10.1007/s11357-020-00262-5>

[6] Marella, M., Seo, B. B., Yagi, T., & Matsuno-Yagi, A. (2009). Parkinson's disease and mitochondrial complex I: a perspective on the Ndi1 therapy. *Journal of bioenergetics and biomembranes*, 41(6), 493–497. <https://doi.org/10.1007/s10863-009-9249-z>

[7] Petzinger, G. M., Walsh, J. P., Akopian, G., Hogg, E., Abernathy, A., Arevalo, P., ... & Jakowec, M. W. (2007). Effects of treadmill exercise on dopaminergic transmission in the 1-methyl-4-phenyl-1, 2, 3, 6-tetrahydropyridine-lesioned mouse model of basal ganglia injury. *Journal of Neuroscience*, 27(20), 5291-5300.

[8] Irwin, I., Finnegan, K. T., Delaney, L. E., Di Monte, D., & Langston, J. W. (1992). The relationships between aging, monoamine oxidase, striatal dopamine and the effects of MPTP in C57BL/6 mice: a critical reassessment. *Brain research*, 572(1-2), 224-231. [https://doi.org/10.1016/0006-8993\(92\)90473-M](https://doi.org/10.1016/0006-8993(92)90473-M)

[9] Kilpatrick, I. C., Jones, M. W., & Phillipson, O. T. (1986). A semiautomated analysis method for catecholamines, indoleamines, and some prominent metabolites in microdissected regions of the nervous system: an isocratic HPLC technique employing coulometric detection and minimal sample preparation. *Journal of neurochemistry*, 46(6), 1865-1876.